ORNL/TM-2000/84

OAK RIDGE NATIONAL LABORATORY

LOCKHEED MARTIN

Characterization of Cassini GPHS Fueled Clad Production Girth Welds

E. A. Franco-Ferreira
M. W. Moyer
M. A. H. Reimus
A. Placr
B. D. Howard

MANAGED AND OPERATED BY
LOCKHEED MARTIN ENERGY RESEARCH CORPORATION
FOR THE UNITED STATES
DEPARTMENT OF ENERGY

ORNL-27 (3-96)

Available electronically from the following source:

Web site www.doe.gov/bridge

Reports are available in paper to the public from the following source.

U.S. Department of Commerce
National Technical Information Service
5285 Port Royal Road
Springfield, VA 22161
Telephone 1-800-553-6847
TDD 703-487-4639
Fax 703-605-6900
E-mail orders@ntis.fedworld.gov
Web site www.ntis.gov/ordering.htm

Reports are available in paper to U.S. Department of Energy (DOE) employees, DOE contractors, Energy Technology Data Exchange (ETDE) representatives, and International Nuclear Information System (INIS) representatives from the following source.

Office of Scientific and Technical Information
P.O. Box 62
Oak Ridge, TN 37831
Telephone 865-576-8401
Fax 865-576-5728
E-mail reports@adonis.osti.gov

ORNL/TM-2000/84

Engineering Technology Division

CHARACTERIZATION OF CASSINI GPHS FUELED CLAD PRODUCTION GIRTH WELDS

E. A. Franco-Ferreira
M. W. Moyer*
M. A. H. Reimus†
A. Placr‡
B. D. Howard‡

*Oak Ridge Y-12 Plant.
†Los Alamos National Laboratory.
‡Westinghouse Savannah River Company.

Date Published: March 2000

Prepared by the
OAK RIDGE NATIONAL LABORATORY
Oak Ridge, Tennessee 37831-6363
managed by
LOCKHEED MARTIN ENERGY RESEARCH CORP.
for the
U.S. DEPARTMENT OF ENERGY
under contract DE-AC05-96OR22464

CONTENTS

Page

LIST OF FIGURES

LIST OF TABLES

CHARACTERIZATION OF CASSINI GPHS FUELED CLAD PRODUCTION GIRTH WELDS

E. A. Franco-Ferreira
M. W. Moyer
M. A. H. Reimus
A. Placr
B. D. Howard

ABSTRACT

Fueled clads for radioisotope power systems are produced by encapsulating $^{238}PuO_2$ in iridium alloy cups, which are joined at their equators by gas tungsten arc welding. Cracking problems at the girth weld tie-in area during production of the Galileo/Ulysses GPHS capsules led to the development of a first-generation ultrasonic test for girth weld inspection at the Savannah River Plant. A second-generation test and equipment with significantly improved sensitivity and accuracy were jointly developed by the Oak Ridge Y-12 Plant and Westinghouse Savannah River Company for use during the production of Cassini GPHS capsules by the Los Alamos National Laboratory. The test consisted of Lamb wave ultrasonic scanning of the entire girth weld from each end of the capsule combined with a time-of-flight evaluation to aid in characterizing nonrelevant indications. Tangential radiography was also used as a supplementary test for further evaluation of reflector geometry.

Each of the 317 fueled GPHS capsules, which were girth welded for the Cassini Program, was subjected to a series of nondestructive tests that included visual, dimensional, helium leak rate, and ultrasonic testing. Thirty-three capsules were rejected prior to ultrasonic testing. Of the 44 capsules rejected by the standard ultrasonic test, 22 were upgraded to flight quality through supplementary testing for an overall process acceptance rate of 82.6%. No confirmed instances of weld cracking were found.

1. INTRODUCTION

The Cassini interplanetary probe to Saturn, launched in October 1997, requires approximately 900 W of electrical power to supply its instruments and components. This power is provided by three radioisotope thermoelectric generators (RTGs); their thermal input comes from iridium alloy-encapsulated $^{238}PuO_2$ pellets. An RTG contains 72 fueled capsules, each producing about 60 W of heat at a clad temperature of 1287°C.

The DOP-26 iridium alloy capsules, shown in Fig. 1, are nominally 29.6-mm outside diameter (OD) by 29.9 mm long and have a wall thickness of 0.68 mm. A 0.44-mm-diam vent at one pole of the capsule, backed by a sintered iridium-frit filter, allows the helium that is a product of the fuel's α-decay to escape. Each capsule consists of two hemishells (or cups) that are joined to each other by a full-penetration, autogenous gas tungsten arc (GTA) girth weld after insertion of the fuel pellet. A band of iridium foil, 0.127 mm thick, is positioned between the fuel pellet and the root side of the weld to shield the pellet from the backside of the weld puddle during welding.

Fuel encapsulation is necessary to maintain the geometric integrity of the brittle fuel pellets throughout the mission. It is also required to limit accidental release of plutonia particles to the

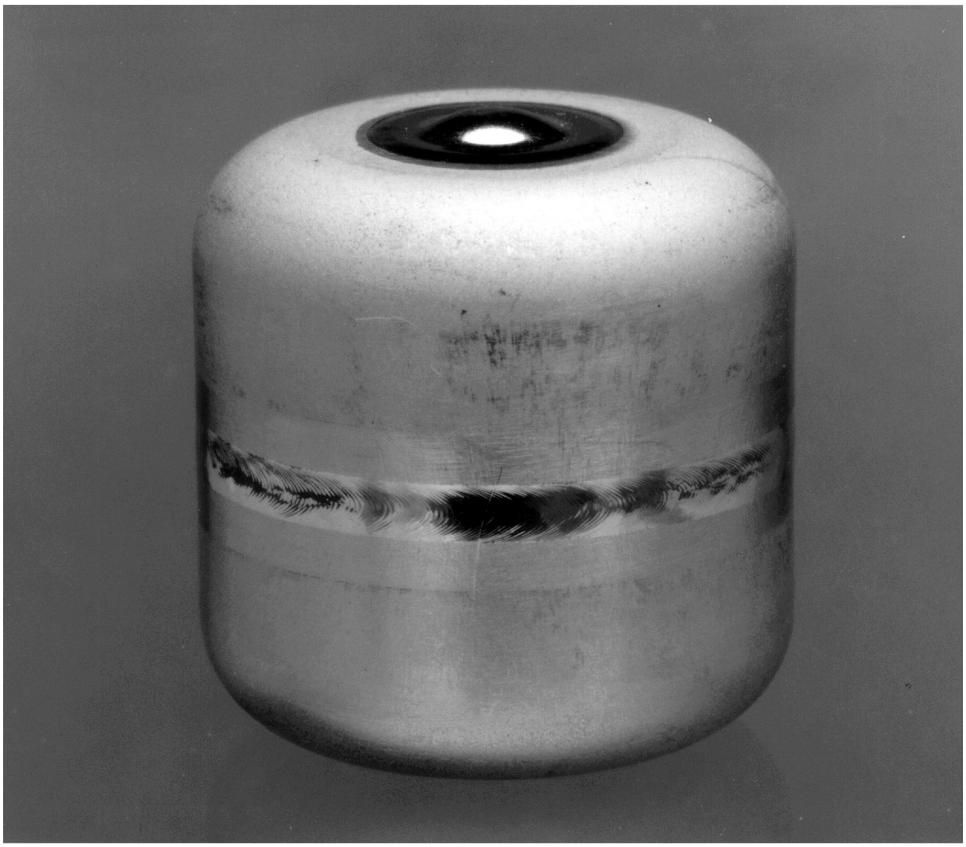

Fig. 1. A typical Cassini heat source capsule.

environment. The two scenarios of most concern entail a launch accident or an inadvertent atmospheric re-entry.

A significant determinant of the capsule's ability to meet its design requirements is the quality of the girth weld. To certify this weld quality, a series of nondestructive examinations (NDEs) was performed on each of the 317 capsules that were fabricated in the course of the Cassini Program.

2. HISTORICAL BACKGROUND

The RTGs used for Cassini are essentially identical to those used on the Galileo Mission to Jupiter, launched in 1989, and the Solar-Polar Ulysses Mission, launched in 1990. The capsule weld quality requirements were as stringent for these two missions as were those for Cassini. However, some difficulties were experienced in meeting the quality requirements for Galileo/ Ulysses.

The optimized iridium alloy used for RTG fuel encapsulation, known as DOP-26, contains by weight 0.3% tungsten, 60 ppm thorium, and 50 ppm aluminum. The thorium dopant serves two important functions. At low levels, it appears that thorium segregates to the grain boundaries and improves grain boundary cohesion; at higher dopant levels, the thorium combines with iridium to form Ir_5Th. These intermetallic precipitates pin the grain boundaries and inhibit grain coarsening while increasing alloy strength at high temperatures, with the optimum dopant level for mechanical properties, not welding, being 200 ppm thorium by weight.[1]

Unfortunately, thorium can contribute to hot cracking in autogenous welds made in DOP-26. The iridium-rich end of the iridium-thorium binary phase diagram shows a eutectic reaction:

$$\text{Liquid} \leftrightarrow (\text{Ir}) + Ir_5Th$$

at 2080°C, and congruent melting of Ir_5Th at 2260°C, both of which occur significantly below the 2454°C melting point of iridium.[2] This behavior would be expected to lead to hot cracking[3] and, in fact, significant problems of this nature were experienced during Galileo/Ulysses production.[4,5]

The DOP-26 material for all three of these missions was produced at Oak Ridge National Laboratory (ORNL). The method used for production of the DOP-26 for the Cassini mission represented a significant improvement over that used for the previous two missions. The specified thorium concentration range was 30–90 ppm. This concentration range is considered to be high enough to achieve the desired grain boundary stabilization and enhanced cohesion effects, yet low enough to avoid significant weld hot cracking.

The DOP-26 sheet produced at ORNL was fabricated into clad vent sets for the Galileo/Ulysses missions at Mound Laboratories in Miamisburg, Ohio. The clad vent sets for the Cassini mission were fabricated at the Oak Ridge Y-12 Plant. A detailed description[6] of this work for the Cassini mission is available.

The Galileo/Ulysses capsules were loaded with fuel and welded at the Savannah River Plant (SRP), now Westinghouse Savannah River Company (WSRC). Early in the program, it was discovered that weld centerline cracking was occurring on the root side of the weld in the overlap region, which is the area between weld tie-in (360°) and where the arc is finally extinguished (450°). A schematic representation of this cracking is shown as a longitudinal section in Fig. 2(*a*) and a transverse section in Fig. 2(*b*).

This cracking was caused by the low-melting (Ir) + Ir_5Th eutectic that, under the influence of normal solidification mechanics, is preferentially segregated to the weld centerline. In the area of the overlap where the second weld pass is less than fully penetrated (i.e., where the welding current has been tapered below maximum), the (Ir) + Ir_5Th eutectic in the unmelted portion of the original weld re-liquefies. The centerline grain boundary separation occurs under the influence of thermal stresses, as well as the mechanical stresses associated with the formation of the tie-in bulge. These root cracks do not propagate into the outer weld layer and, hence, are not visible on the completed capsule.

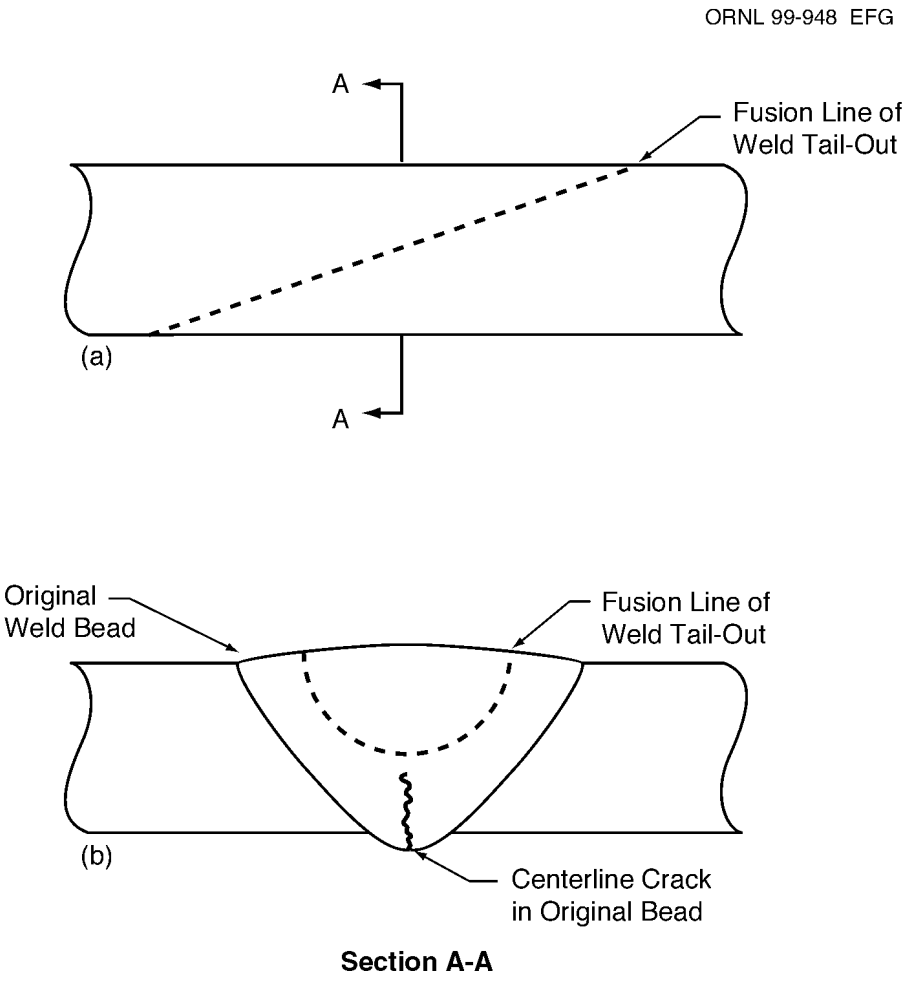

Fig. 2. Schematic drawing of Galileo/Ulysses weld cracking.

A significant number of cracks, produced by the mechanism discussed above, were discovered in the early stages of Galileo/Ulysses capsule production. One contributor was the melting practice, which was not as well controlled as it was on the Cassini Program. Further, the postmelting analytical techniques for thorium concentration had an accuracy of ±50%. This necessitated the development of ultrasonic testing (UT) equipment and procedures that could reliably detect the cracks. This test was also expected to verify the absence of cracks once improvements[7] were introduced into the production of the DOP-26 material and into the welding procedure.

The ultrasonic inspection system developed by SRP was designed to hold the capsule with its axis of rotation in a horizontal plane. An arm held the transducer at a fixed angle and was positioned to perform a single circumferential scan of the capsule. The axial position of the transducer was adjusted manually. Fig. 3 is a schematic of the setup. A 5.0-MHz KB-Aerotech gamma transducer with a 19.05-mm focal length in water was used for the inspection. An Automation Industries S-80 instrument was used for data acquisition. The transducer was mounted with its axis tilted 31° from the normal to the capsule surface. This angle is just past the

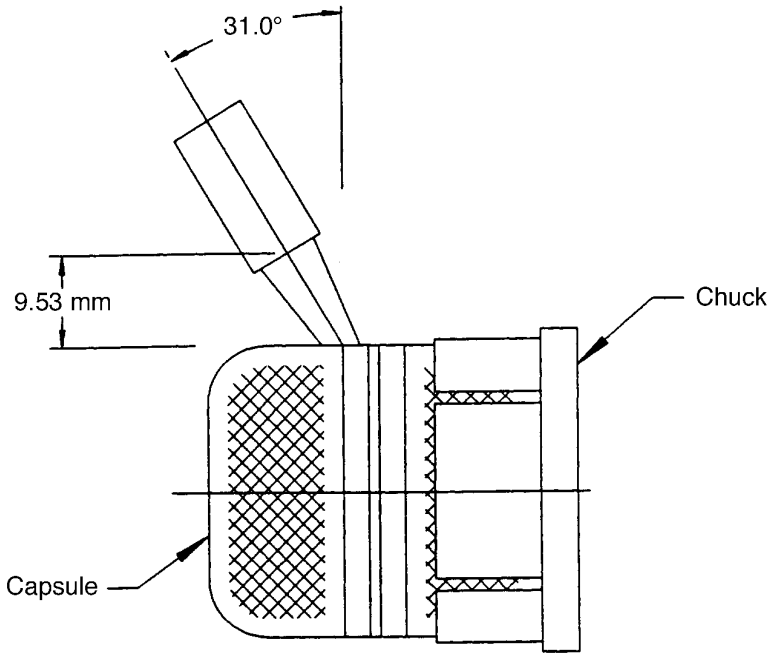

Fig. 3. Setup for Galileo/Ulysses production ultrasonic inspection.

shear critical angle for iridium and produced Rayleigh waves in the capsule. Instrument output was displayed on a strip chart recorder. For the inspection, only a single reference slot was used to calibrate the instrumentation. Although this system was difficult to set up and adjust, it was successfully used for ultrasonic inspection throughout Galileo/Ulysses production.

It was determined at the inception of work on the Cassini Program that the Galileo/Ulysses threshold was set by adjusting the S-80 instrumentation so that the signal from a 0.152-mm deep × 0.254-mm wide × 1.27-mm long electrodischarge machined (EDM) slot produced a full-scale output. The rejection threshold was then set at 80% of full-scale, and this level was designated to be a “No. 8” signal.

The SRP data[8] indicate that the signal generated by a “No. 8” reflector was approximately equal to that from a reflector with an area of 0.173 mm2. This is equivalent to a 1.27-mm-long slot that is 0.135 mm deep. Subsequent experiments at the Y-12 Plant showed that at 5.0 MHz a constructive interference occurs in the signal from a 0.076-mm-deep by 0.254-mm-wide slot that causes it to be almost as large as the signal from a 0.152-mm-deep slot.

Although the Galileo/Ulysses ultrasonic inspection system had the above-mentioned shortcomings, it was successfully employed throughout the production program at SRP. A total of 615 welded iridium cup-sets were used to produce 447 flight-quality GPHS capsules. This represents an overall net process yield of 72.7% (Ref. 9).

At the start of the Cassini Program the ultrasonic instrumentation at SRP was determined to be obsolete, and the tooling and fixturing for capsule inspection were no longer available. This, coupled with the fact that capsule production was moved from WSRC to Los Alamos National Laboratory (LANL), necessitated the development of a new ultrasonic inspection system and procedure for the Cassini Program.

3. WELD DEFECTS AND ANOMALIES

Weld defects are normally defined as conditions that reduce the cross-sectional area of the weld and thereby its ability to resist the stresses for which it has been designed. On the other hand, weld anomalies are usually geometric inconsistencies that do not affect the weld's ability to perform as designed.

A transverse cross section of a normal DOP-26 heat source capsule girth weld is shown in Fig. 4. Welds of this type are subject to defects that are shown schematically in Fig. 5(*a*)–(*e*). The two most serious of these defects are planar in form and run longitudinally along the weld. The first, shown in Fig. 5(*a*)**,** is a centerline root crack. Lack of fusion/penetration, shown in Fig. 5(*b*), is geometrically similar to the root crack and is an equally severe stress concentration. Excessive porosity, shown in Fig. 5(*c*), does not produce as sharp a stress concentration as a planar defect but is still undesirable beyond a certain minimum level. Weld root suck-back, shown in Fig. 5(*d*)**,** while not as severe a stress concentration as a root crack or lack of penetration, can still compromise the weld's load-carrying ability. None of these defects can be detected by visual examination of the outer surface of the capsule. Thus, ultrasonic testing and/or radiography (RT) must be used.

The final cross section-reducing defect, shown in Fig. 5(*e*), is undercut. This defect, which is apparent on visual inspection, is rarely, if ever, encountered with a properly developed automatic welding procedure such as that used on the Cassini capsules.

Three conditions, which can be termed geometric weld anomalies, are capable of producing ultrasonic signals that are difficult to distinguish from those produced by the defects discussed above. These anomalies, shown schematically in Figs. 6(*a)*–(*c*), do not normally compromise the weld's integrity insofar as the minimum wall thickness requirement is met. However, the existence of these types of anomalies was responsible for a significant complication in the NDE of the Cassini girth welds.

The first of these anomalies, weld shield fusion, shown in Fig. 6(*a*), results when the molten metal on the root side of the weld puddle touches and fuses to the iridium foil weld shield. This condition, although normally intermittent, can extend for a significant portion of the capsule circumference. The ultrasonic signals returned by the corners that are formed by the intersection of the weld root and the shield are identical to those from a planar weld defect.

Because of crystallographic textures during forming, the wall thickness of the capsule hemi-shells varied by up to ±8.1% around the circumference.[10] The welding setup utilized tooling rings with a precise inside diameter of 29.768–29.819 mm. These rings surrounded the cups and forced all the cup-to-cup mismatch to the inside wall. In a situation in which a

ORNL 99-1033 EFG

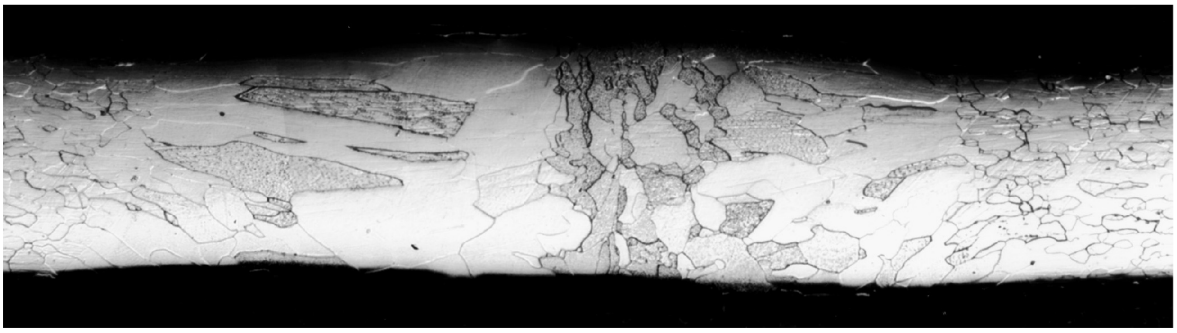

Fig. 4. Transverse cross section of a normal iridium capsule girth weld (46×).

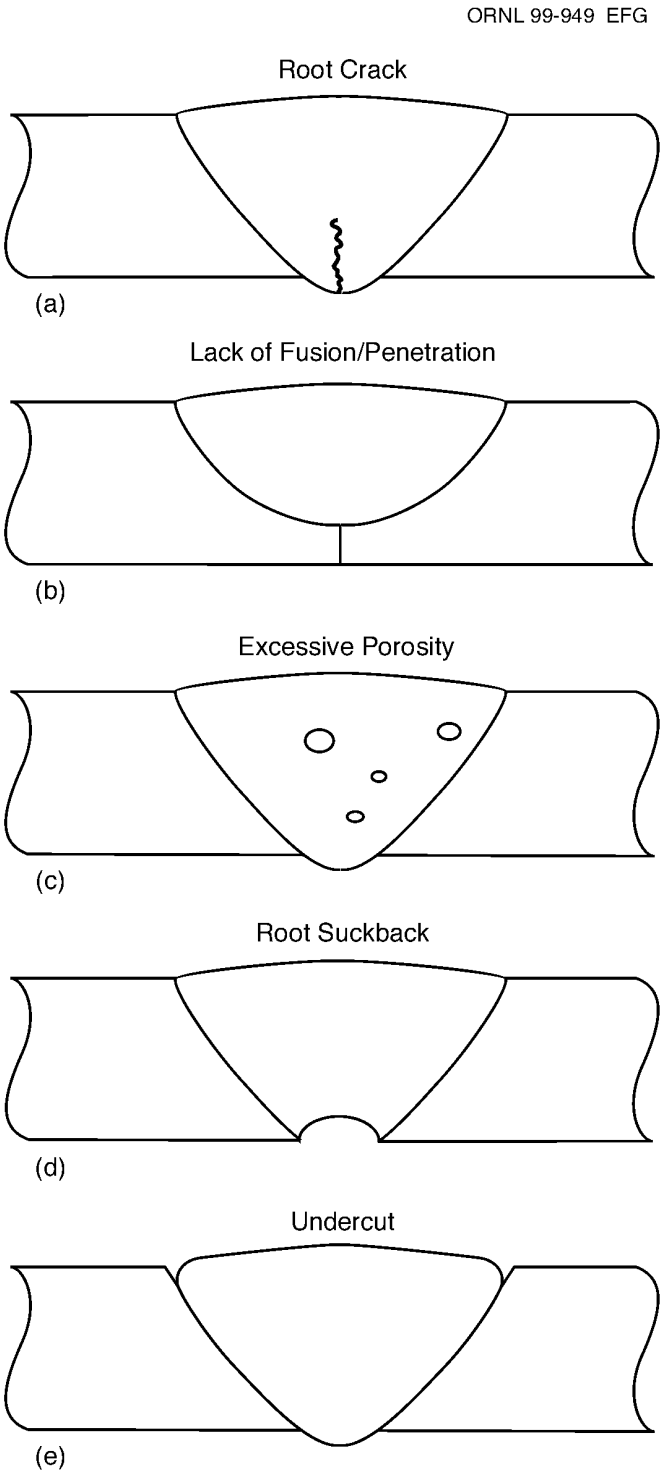

Fig. 5. Rejectable weld defects.

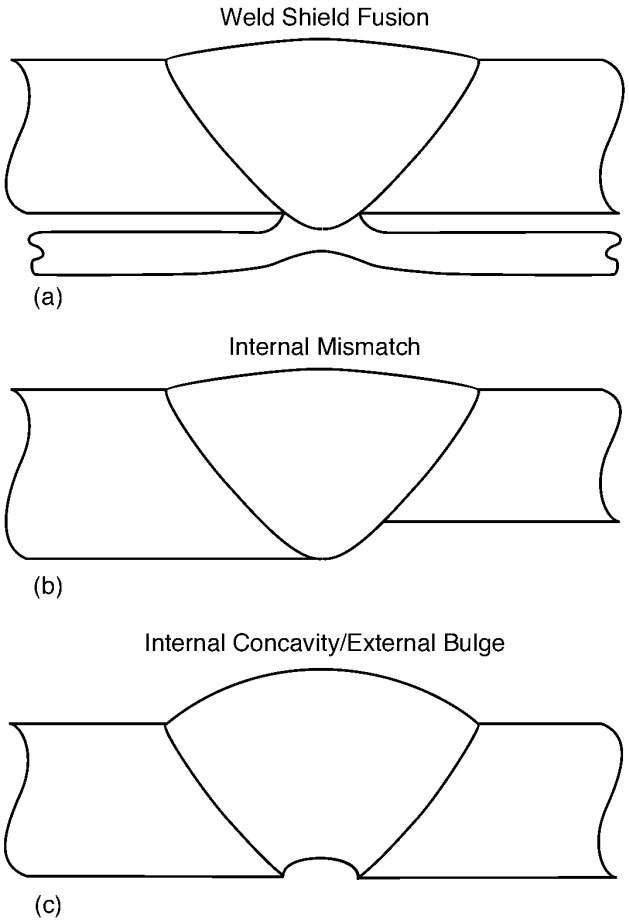

Fig. 6. Geometric weld anomalies.

maximum/minimum tolerance stack-up is situated directly across the joint, a condition such as that shown in Fig. 6(*b*) can result. Once again, a corner that can produce a relatively large ultrasonic return is created.

The Cassini cups each had a notch, nominally 0.30 mm wide by 0.175 mm high, located on the weld joint. These notches were aligned prior to welding to produce a single vent notch, which was nominally 0.30 mm wide by 0.35 mm high. The purpose of this notch, which was closed over at weld tie-in, was to prevent weld blowout due to internal pressure buildup during welding. Welding current taper-out was initiated at the moment of weld tie-in and continued for 127° (33 mm) past the vent slot. Because the internal pressure continued to increase after vent slot closure, there was invariably a slight bulge at the tie-in area. This condition is shown in Fig. 6(*c*). There is no deleterious effect from this bulge as long as the weld thickness is not reduced below the minimum requirement. There is no minimum weld thickness specified on the drawings. However, the drawing requirement for minimum wall thickness on the cups is 0.55 mm. Thus, it can be inferred that the minimum weld thickness should not be below this value. Excessive bulging results in a rejection by a go/no-go ring gauge, and it has also been shown[11] that this condition is normally accompanied by unacceptable weld thinning. However, as can be seen in Fig. 6(*c*), the corners created at the edges of the internal concavity are strong reflectors and can

produce an ultrasonic signal that must be discriminated from that of a rejectable defect even in capsules that pass the ring gauge.

4. NDE DEVELOPMENT

As mentioned previously, the obsolescence and unavailability of the SRP Galileo/Ulysses inspection system necessitated the procurement of new equipment and calibration standards. A collaborative effort was undertaken by WSRC and Y-12 Plant personnel, under Y-12 lead, to conceptualize and specify a new and improved ultrasonic inspection system. In early 1990 a purchase specification for four identical new ultrasonic inspection systems was prepared by the Y-12 Plant with review and concurrence by WSRC and LANL. The intent was to have one system each at the Y-12 Plant and WSRC for development work and two systems at LANL for production inspection (one in a hot area and one in a cold area).

The inspection systems consist of three motorized axes. These are capsule rotation (θ), a gimbal for transducer angular position, and a vertical (Z) axis for transducer scanning. In addition, there were two manually driven micrometer axes (X and Y) for horizontal positioning of the transducer. The 30-MHz bandwidth pulser/receiver gated-peak-detectors provide ultrasonic data acquisition. The systems are controlled by Type 486 computers and appropriate software. The software enables saving and plotting the data and is driven by a macro file to perform a menu of specific user-defined tasks. The macro file aids in repeatable inspection and setup for GPHS calibration standards and production parts. An overall view of one of the production inspection systems located at LANL is shown in Fig. 7.

ORNL 99-1025 EFG

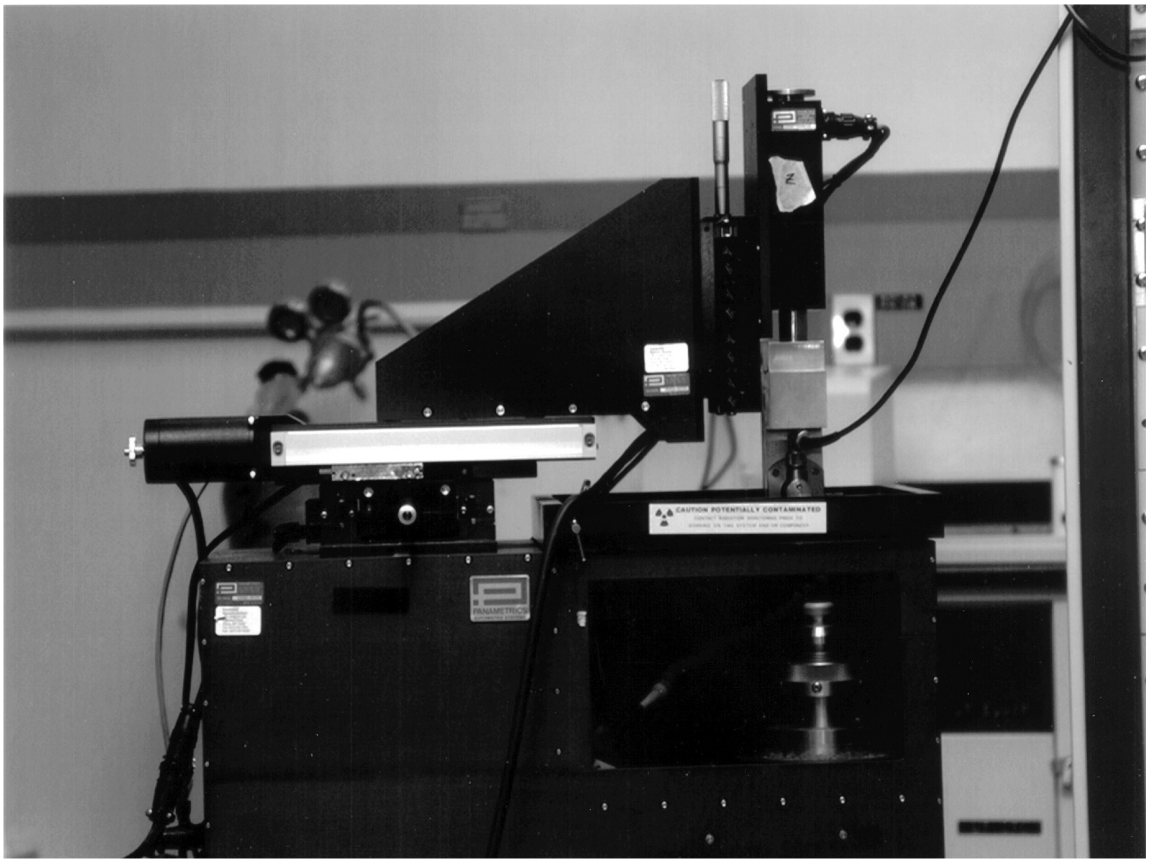

Fig. 7. Panametrics automated UT immersion system for Cassini NDE.

Four empty iridium capsules were welded at WSRC for use as ultrasonic calibration standards. This was necessary because the calibration standard(s) used during Galileo/Ulysses production could not be safely used because of radioactive contamination. Furthermore, archival information suggested that the Galileo/Ulysses calibration standard(s) probably did not have slots that covered a comprehensive size range. To better quantify defect size, several reference slots with dimensions that span the range of expected defect sizes should be used for calibration. This approach verifies the linearity of the instrumentation and provides confidence in the testing procedure. The calibration capsules were welded at WSRC on an existing laboratory welding system that had been used in the Galileo/Ulysses program. Because of welding setup problems, the capsules had unacceptably large bulges at their tie-in regions. However, they were deemed to be adequate for initial development and testing work and were shipped to the Y-12 Plant to have the appropriate slots machined (EDM) into their inside surfaces. Slot dimensions and locations are given in Table 1, and the slot configurations are shown schematically in Fig. 8. The weld bulges that interfered with signal interpretation were located between 0° and 90°.

Initial development work[12,13] with the new inspection systems and the calibration standards discussed above used a nominal 31° (from the normal) angle of incidence for the transducer (the same as that used in Galileo/Ulysses). This setup, as in the Galileo/Ulysses case, produced a surface (Rayleigh) wave in the capsule wall. The frequency was changed from 5.0 to 3.5 MHz to improve the system's performance in detection of the slot sizes of interest. This frequency change resulted in less noise and greater penetration power.

The initial inspection procedure called for four scans to be made for each ultrasonic inspection: a top scan, a bottom scan, a left tangential scan, and a right tangential scan. These are shown schematically in Fig. 9. The top and bottom scans were sensitive to defects oriented parallel to the weld centerline, while the tangential scans were sensitive to those oriented perpendicular to the weld. The maximum amplitude signals from each pair of scans were used to determine defect size.

Unfortunately, the 31° technique, which is shown schematically in Fig. 10, proved to be difficult to use and interpret. This was primarily because an angled entry surface echo is unstable in amplitude and position. Added to this instability were surface geometrical variations at the

Table 1. Dimensions of slots in initial Cassini calibration standards

Slot No.	Location (deg)	Orientation	Depth (mm)	Width (mm)	Weld CL distance (mm)
1	0	Vertical	0.051	0.102	3.81
2	30	Vertical	0.076	0.102	3.81
3	60	Vertical	0.152	0.102	3.81
4	90	Vertical	0.229	0.102	3.81
5	120	Vertical	0.152	0.102	0.762
6	150	Horizontal	0.076	0.102	0.762
7	180	Horizontal	0.152	0.102	0.762
8	210	Horizontal	0.076	0.254	3.81
9	240	Horizontal	0.051	0.102	3.81
10	270	Horizontal	0.076	0.102	3.81
11	300	Horizontal	0.152	0.102	3.81
12	330	Horizontal	0.229	0.102	3.81

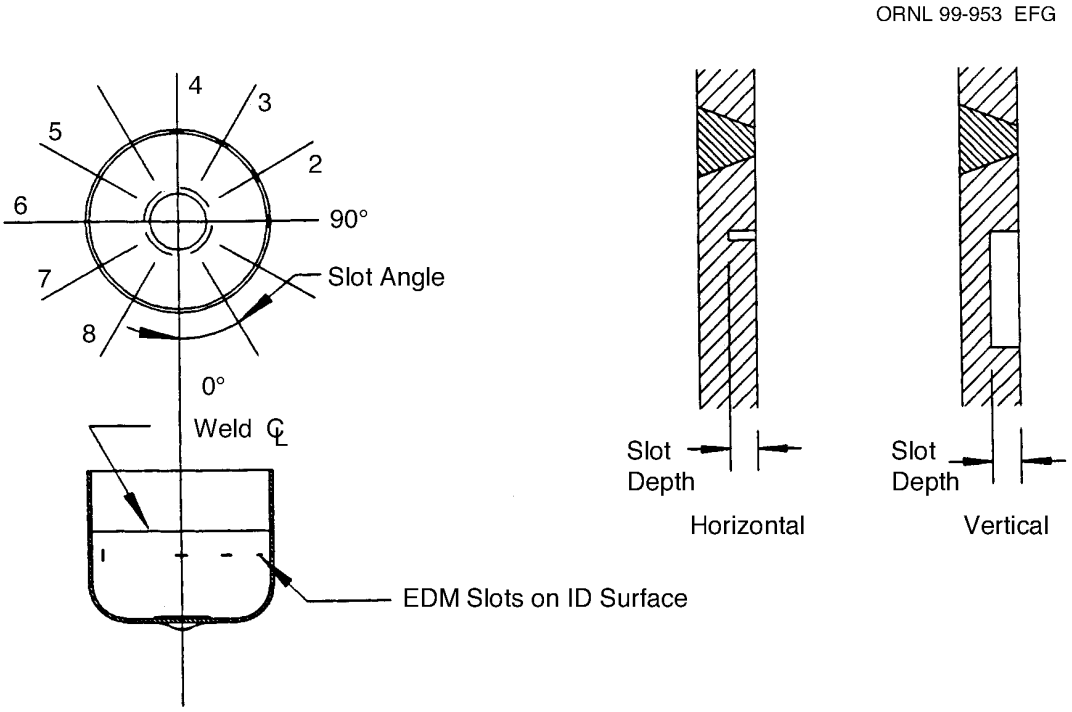

Fig. 8. Slot configurations in initial Cassini calibration standards.

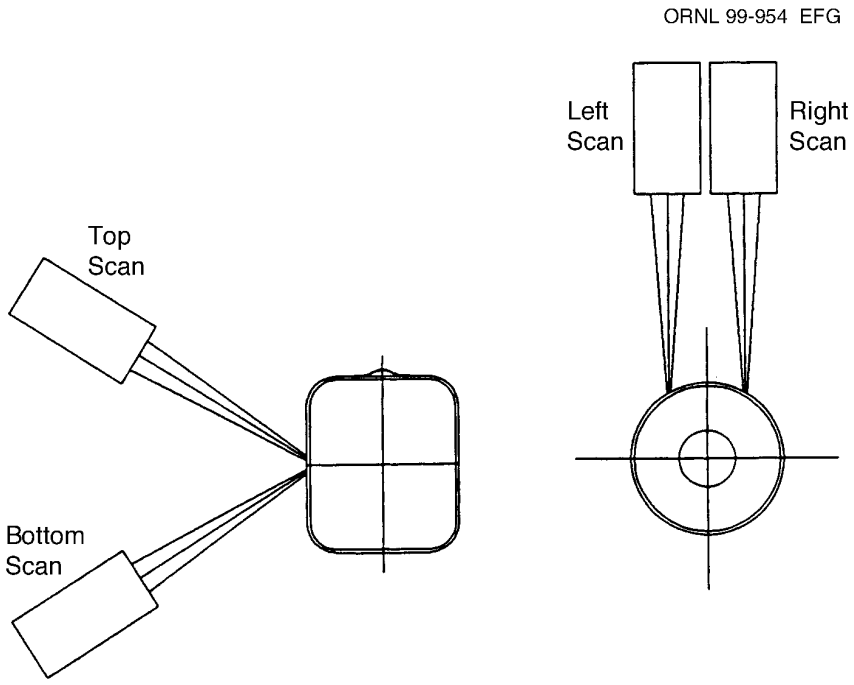

Fig. 9. Initial setup for Cassini ultrasonic inspection development.

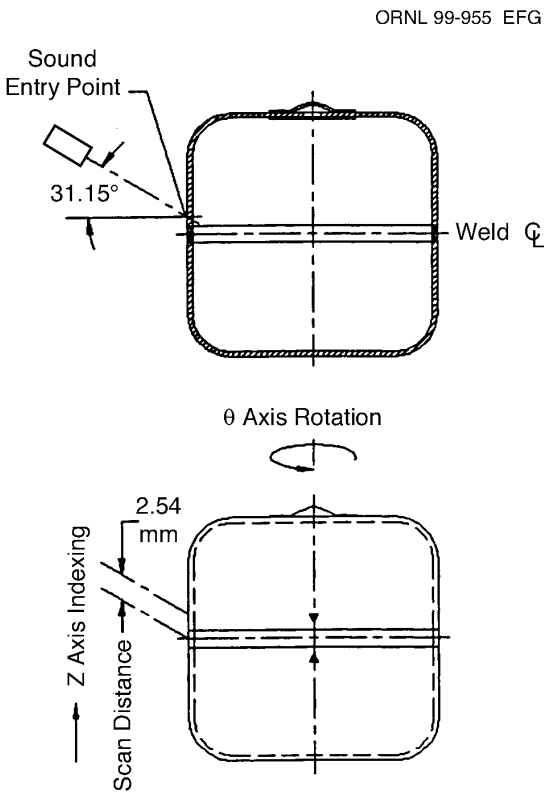

Fig. 10. 31° Rayleigh wave technique for Cassini ultrasonic inspection development.

sound entry point, which was essentially at the weld fusion line. Furthermore, there was inadequate separation between the entry and the defect echoes, as shown in Fig. 11. In addition to lack of signal separation, this technique produced excessive background noise. This is illustrated in Fig. 12, which is an actual C-scan display of the notches in a calibration standard. The dark areas in this and subsequent, similar, figures represent ultrasonic returns.

Work[13] at WSRC, which explored a wide range of incidence angles, led to a refined technique that employed a 39° incidence angle. This angle resulted from shifting the sound entry point away from the weld to the much more geometrically stable curved shoulder of the capsule, as shown in Fig. 13. This angle provided the first useful Lamb wave operational mode. This technique achieved the enhanced signal separation shown in Fig. 14. A C-scan display using this technique is shown in Fig. 15. The same calibration standard as used for Fig. 12 produced this display. The background noise was significantly reduced, and the responses from the notches were much more discernible.

A final refinement of the technique was to scan only the top end surface of the capsule with the axis of the transducer parallel to the capsule's rotational axis. This orientation automatically selects the optimum incidence angle of 19.52° from the vertical (70.48° from horizontal) as shown in Fig. 16. Signal separation is further enhanced, as shown in Fig. 17. The top-scan data display for the same standard as used above is shown in Fig. 18. Two scans, one with the vent up and one with the vent down, are necessary for a complete capsule inspection.

The inspection systems were modified to accommodate the top-scan technique. This simple change consisted of repositioning the motorized Z-axis drive to the X-axis, which allowed an automated scan over the path shown in Fig. 16. The transducer gimbal was fixed in the vertical

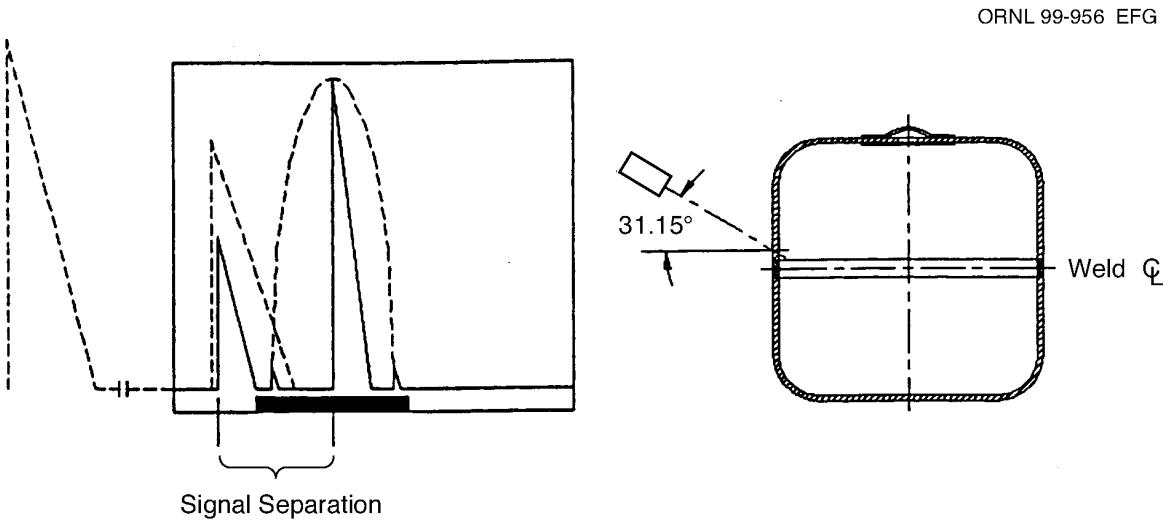

Fig. 11. Schematic of signal configuration from 31° Rayleigh wave technique.

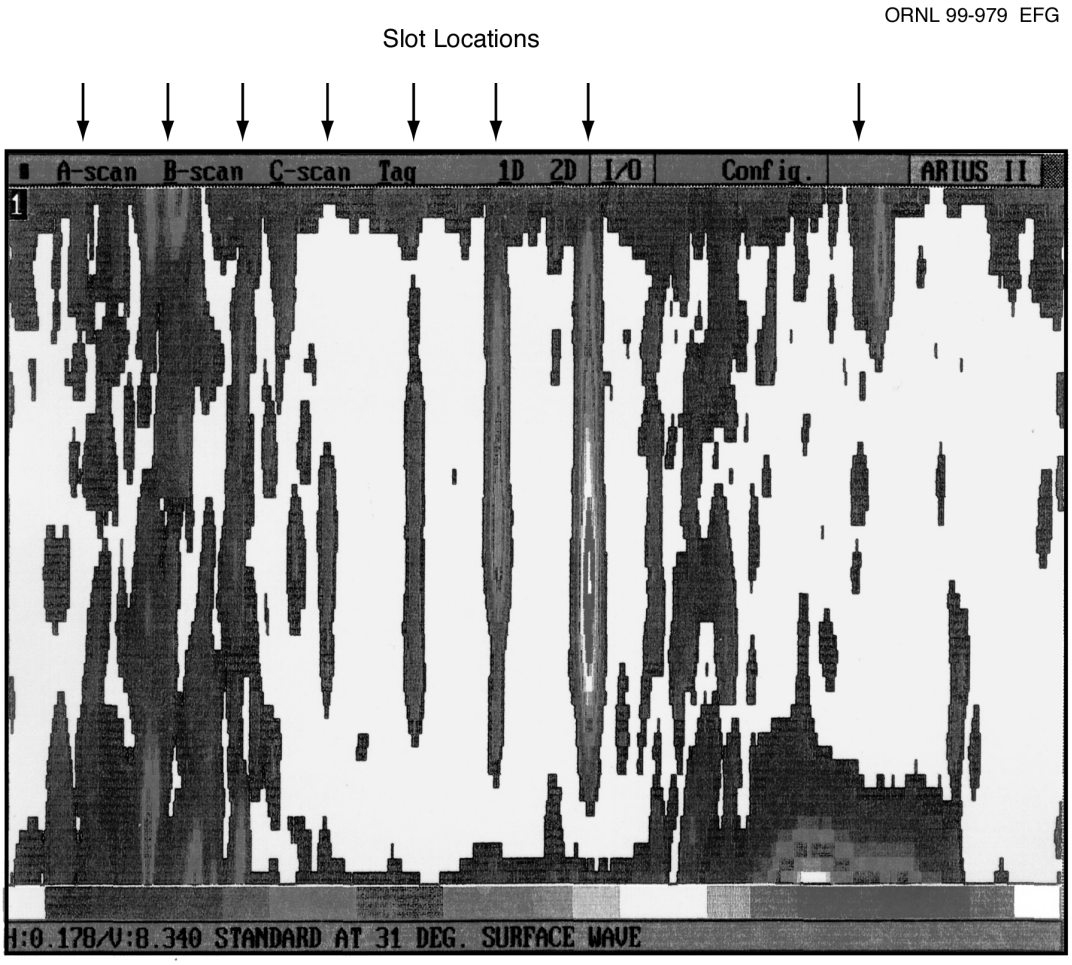

Fig. 12. C-scan display of Rayleigh wave 31° scan of calibration standard No. 47.

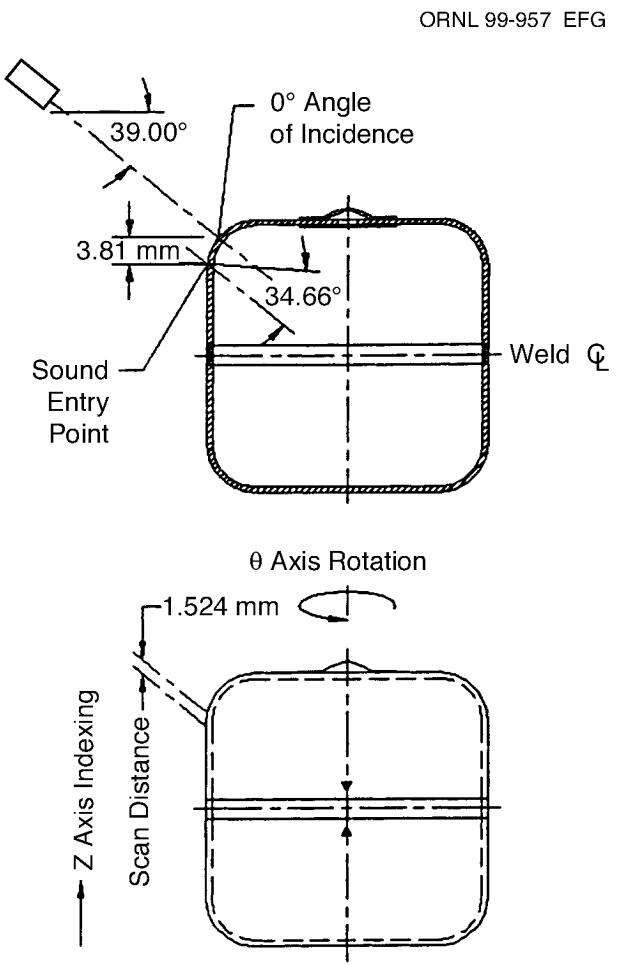

Fig. 13. 39° Lamb wave technique for Cassini ultrasonic inspection development.

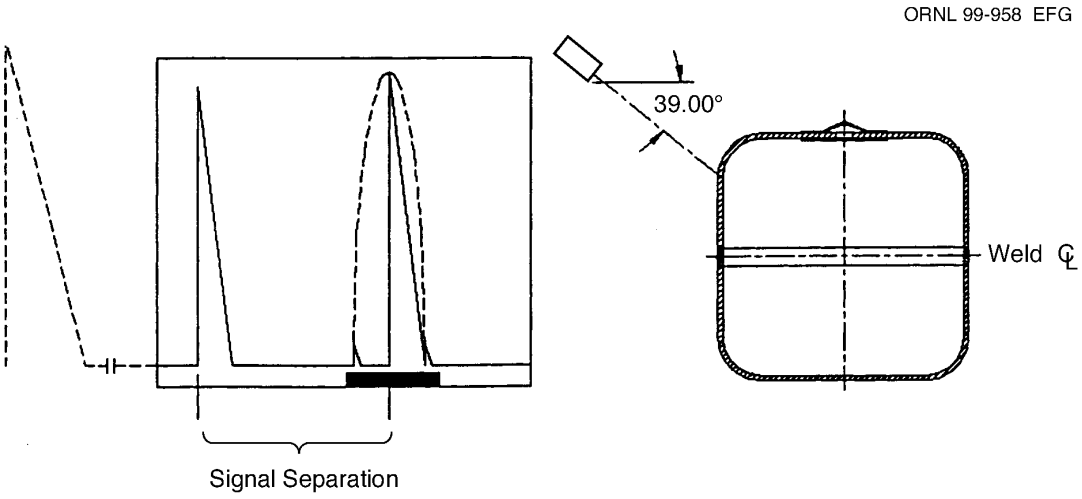

Fig. 14. Schematic of improved signal separation from 39° Lamb wave technique.

ORNL 99-980 EFG

Fig. 15. C-scan display of Lamb wave 39° scan of calibration standard No. 47.

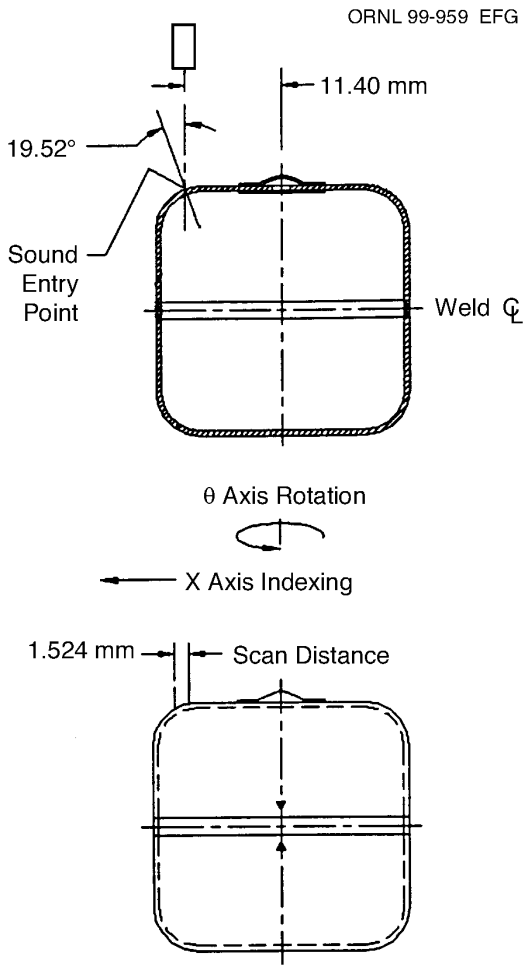

Fig. 16. Top-Scan Lamb wave technique for Cassini production ultrasonic inspection.

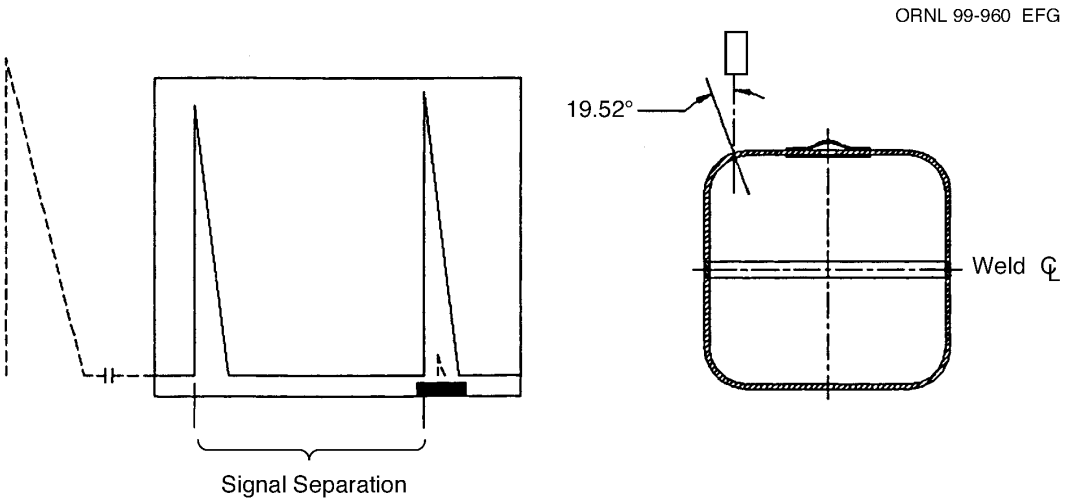

Fig. 17. Schematic of signal separation and noise reduction from top-scan Lamb wave technique.

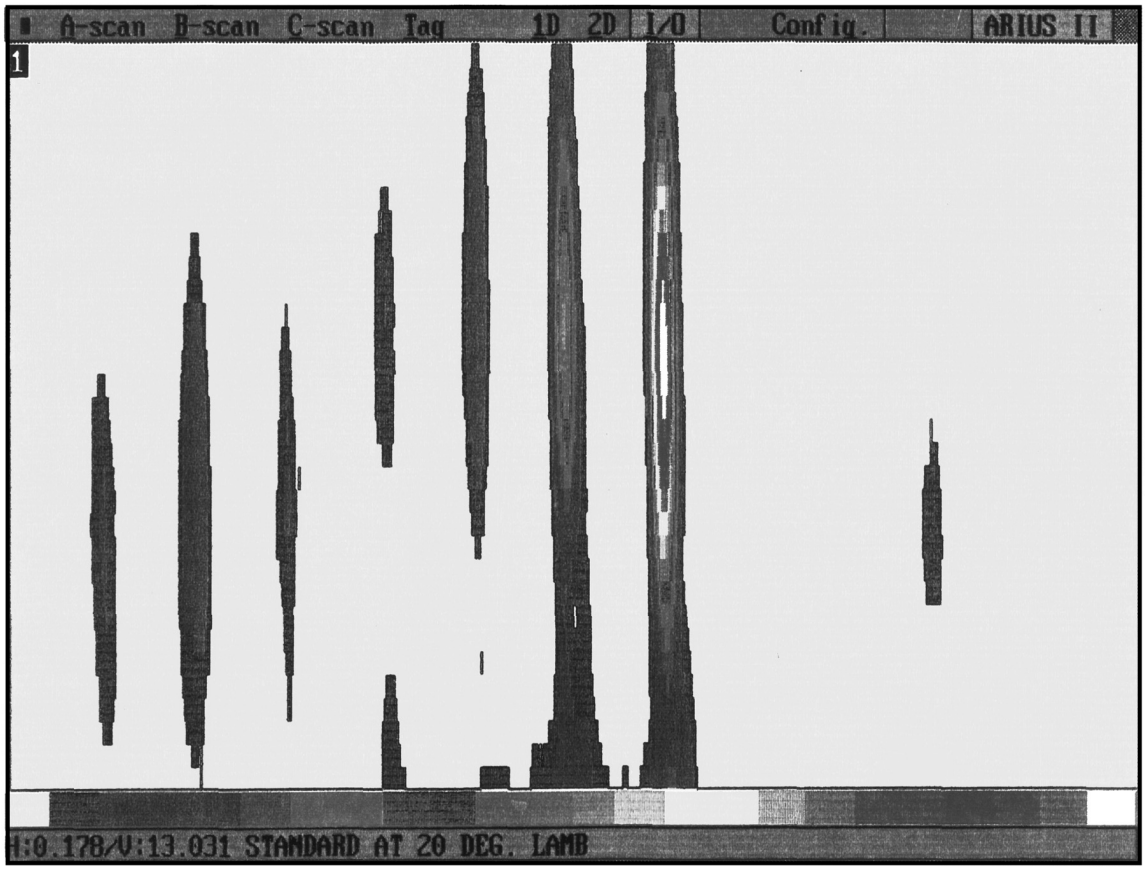

Fig. 18. C-scan display of Lamb wave top-scan of calibration standard No. 47.

position, and the micrometer Y-axis was retained for fine adjustment transverse to the scan axis. The ultrasonic instrumentation was also modified to provide a 100-MHz digitizer to acquire full waveforms as well as the gated peak detection. This enabled the system to measure the time-of-flight of the detected ultrasonic signals and to provide a B-scan display as well as the standard C-scan display.

The top-scan technique proved to have many advantages over those tried previously. Among these advantages are

- simple system and part setup,
- excellent repeatability,
- stable entry surface echo,
- weld centerline easily located,
- maximized signal separation,
- minimized background noise,
- simple gate setup,
- minimized gate width, and
- lowest sensitivity to geometric reflectors.

This technique was approved at a meeting of the heat source community for Cassini production inspection on April 15, 1993, and was subsequently used for all flight-quality hardware.

To improve the implementation of the top-scan technique, a new set of calibration standards was made. These calibration standards were welded in such a way that no tie-in bulges were present. Initially, each calibration standard had eight slots machined (EDM) into its inner surface. Slot configurations were similar to those shown in Fig. 8. Their dimensions and placements are shown in Table 2.

The slot sizes were chosen to have a better distribution around the go/no-go equivalent slot depth of 0.13 mm (0.00512 in.) than did those in the first set of calibration standards.

With the perfection of the top-scan technique, five additional slots were added to the new calibration standards, and these standards were then used for all production inspections. The dimensions and placements of these additional slots are shown in Table 3.

These slots enabled a calibration of the flaw distance from the weld centerline. As will be seen, this capability was important in discriminating between true weld flaws and geometric anomalies.

The development work discussed above was successful in providing equipment and techniques capable of detecting root cracks, lack of fusion/penetration, and root suckback with a

Table 2. Dimensions of slots in new calibration standards

Slot No.	Location (deg)	Orientation	Depth (mm)	Weld CL distance (mm)
1	90	Horizontal	0.076	3.81
2	120	Horizontal	0.114	3.81
3	150	Horizontal	0.152	3.81
4	180	Horizontal	0.203	3.81
5	240	Vertical	0.076	3.81
6	270	Vertical	0.114	3.81
7	300	Vertical	0.152	3.81
8	330	Vertical	0.203	3.81

Table 3. Dimensions of additional slots in new calibration standards

Slot No.	Location (deg)	Orientation	Depth (mm)	Weld CL distance (mm)
9	210	Horizontal	0.127	0.000
10	255	Horizontal	0.127	–1.803
11	285	Horizontal	0.076	1.753
12	315	Horizontal	0.127	1.753
13	345	Horizontal	0.178	1.753

high level of sensitivity. Furthermore, the accept/reject criteria were well correlated to those used on the Galileo/Ulysses program. Thanks to the top-scan procedure, testing was carried out on individual fueled capsules in a short time, which was an important consideration for meeting the as low as reasonably achievable (ALARA) personnel radiation exposure requirements.

Unfortunately, the ultrasonic test proved to be incapable of unequivocally discriminating between the planar (and most deleterious) defects shown in Figs. 5(*a*) and (*b*) and the less severe area-reducing defects shown in Figs. 5(*c*) and (*d*). In addition, the standard gated peak detection ultrasonic inspection was unable to identify and separate the benign geometric anomalies shown in Figs. 6(*a*)–(*c*). With the time-of-flight capability, some of these benign defects could be identified by using an additional data scan that acquired full waveforms. However, the ultrasonic inspections were not able to identify and separate benign from deleterious conditions in all cases. The implication of this lack of discrimination in the ultrasonic test is the possibility of an unnecessarily high rejection rate for capsules with no harmful defects. This situation established the need for additional development work on enhanced/alternate inspection methods that could separate the nonrelevant from the relevant indications identified by the ultrasonic scans.

The most commonly occurring nonrelevant condition was weld shield fusion, shown schematically in Fig. 6(*a*). The mechanism for the creation of weld shield fusions has been touched on previously. A more detailed analysis of the problem follows.

Two weld shield configurations were used during the Cassini heat source production. The first design, which was identical to that used in Galileo/Ulysses, entailed having the weld shield attached to the inner wall of the unvented cup (the shield cup) by tab welds at three locations. A drawing of this weld shield, as installed, is shown in Fig. 19. Based on drawing tolerances, the

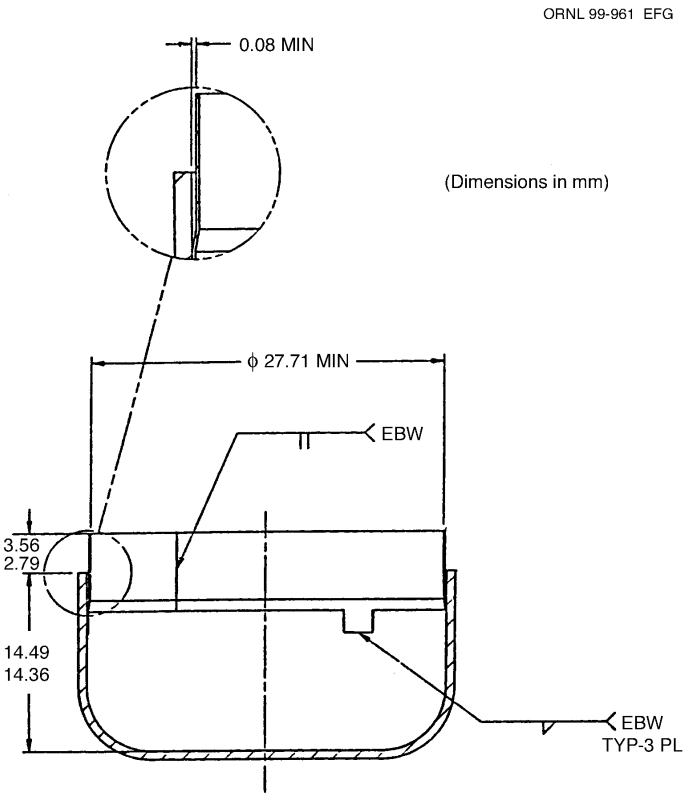

Fig. 19. Galileo/Ulysses weld shield and shield cup.

radial gap between the outer surface of the weld shield and the inner surface of the shield cups ranged from 0.08 to 0.36 mm. These dimensions are based on an assumption of complete roundness and concentricity in the cups and shields. This is a condition that rarely, if ever, existed. Only 6 of the 317 capsules had Galileo/Ulysses-configuration weld shields, but none of these were shipped as flight-quality hardware for the Cassini Program.

A new weld shield design, termed Type II, evolved during the early stages of welding development on the Cassini Program. This shield, shown in Fig. 20, was a separate piece designed to wrap snugly around the fuel pellet with a small amount of overlap at the shield ends. A radial offset of 0.152 mm running circumferentially around the middle of the shield provided spacing away from the cups' inner surfaces. This radial gap, based on drawing tolerances, ranged from 0.08 to 0.57 mm. Once again, this spacing could not be expected to be uniform all around the circumference.

Because of the ±8.1% wall thickness variation in the cups mentioned earlier, it was necessary to develop a welding procedure that ensured slight overpenetration for the thickest portions of the cup walls. Thus, conditions were conducive to weld shield fusion, especially in instances of minimal radial gap and/or off-center pellet/shield positions. In fact, during the course of welding procedure and NDE development, weld shield fusion was found to be a common occurrence. It ranged in severity from a mild sticking-type adherence (like a diffusion bond) over a short distance to complete fusion, such as that shown in Fig. 21, which could extend for a significant distance. In contrast, the configuration of an unfused weld shield is shown in Fig. 22. The entire range of weld shield fusions produced definite ultrasonic signals, many of which were above the rejection level. The frequency of weld shield fusions verified that the weld shield performed its intended function of preventing contact of the weld root with the fuel pellet.

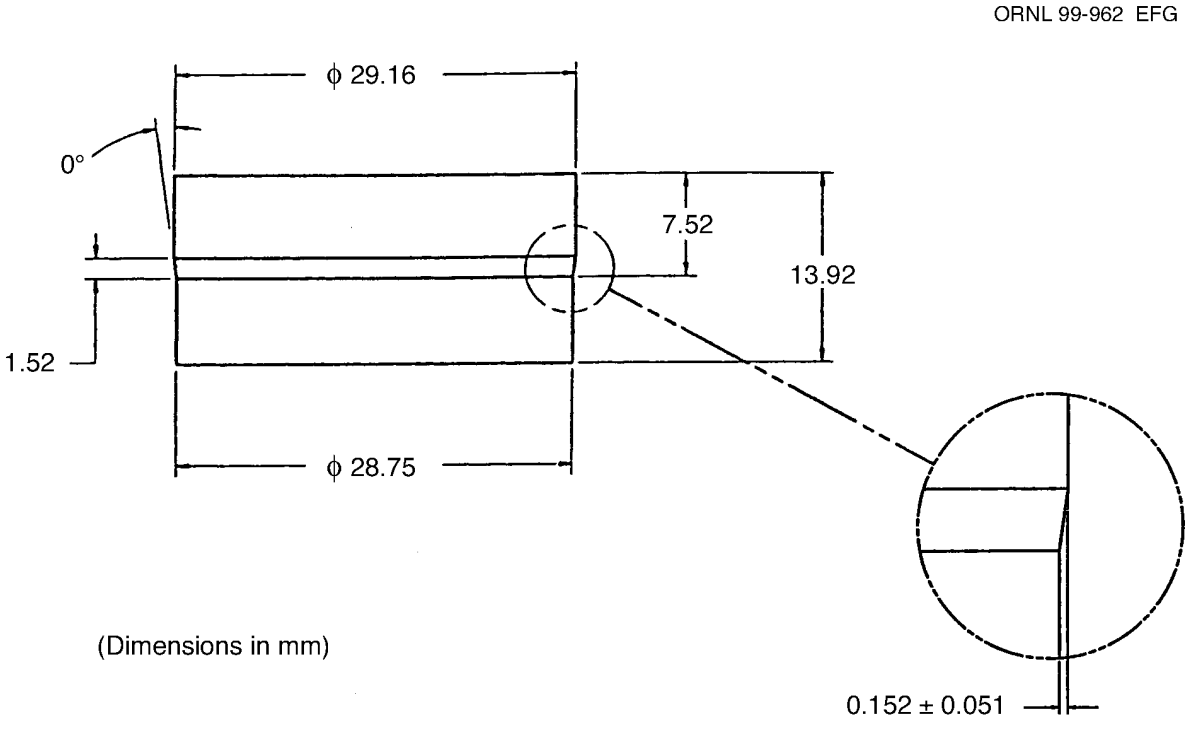

Fig. 20. Cassini Type II weld shield design.

ORNL 99-1026 EFG

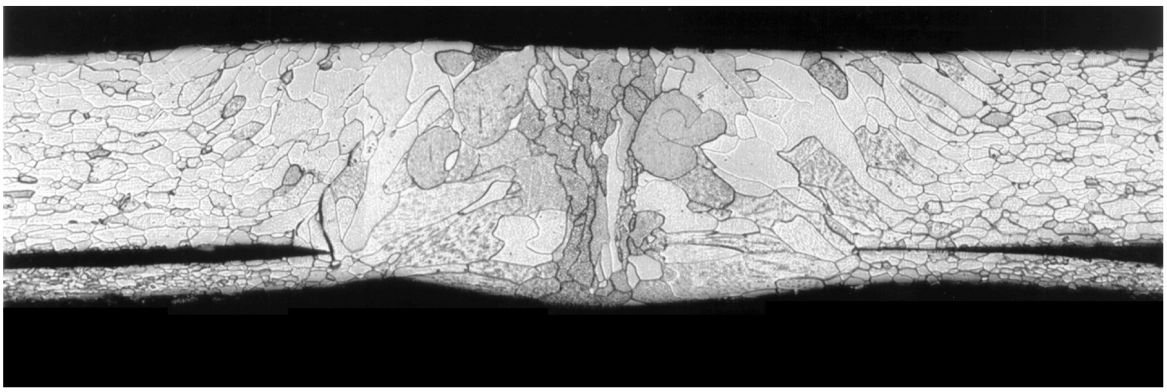

Fig. 21. Transverse cross section of a weld shield fusion (47×).

ORNL 99-1044 EFG

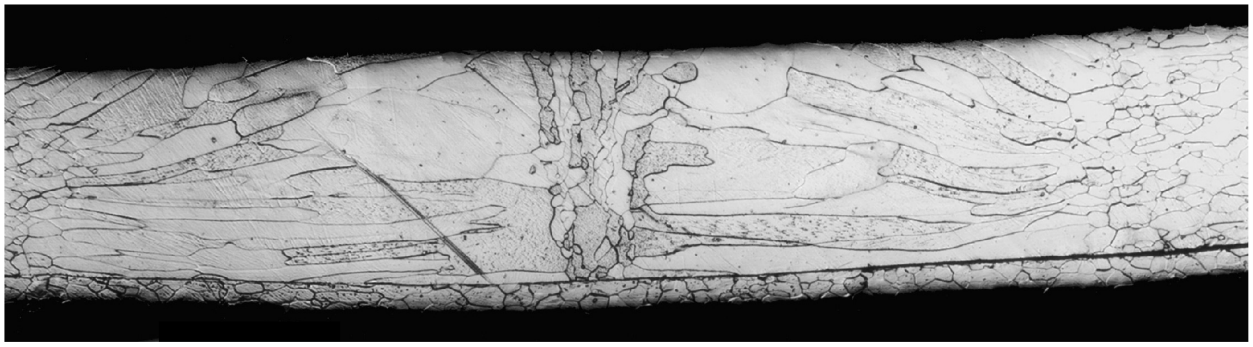

Fig. 22. Capsule girth weld backed by an unfused weld shield (46×).

A possible improvement to weld shield installation would be to wrap the Type II shield very tightly around the fuel pellet and keep it that way. This would maximize the spacing of the shield away from the weld root. An example of an approach to this is shown in Fig. 23 in which a Type II weld shield has been laser welded tightly around a simulant fuel pellet.

As Fig. 6(*a*) shows, the geometric reflectors produced by weld shield fusion are displaced from the weld centerline. By using a time-of-flight analysis on the reflected signal, it was possible to determine the distance of a reflector from the weld centerline. However, this technique was not developed with sufficient confidence to provide unequivocal identification of weld shield fusions in time for Cassini production inspection.

An attempt was made to apply an artificial intelligence pattern recognition software package (ICEPAK) to the geometric reflector problem. This system proved to be quite effective in pattern recognition. However, its use depends on an extensive “learning” regimen that requires the input of large quantities of data from actual destructive physical tests on numerous sample reflectors. Because of the high cost and paucity of actual iridium capsule samples that could be destructively analyzed, it was not possible to implement ICEPAK for Cassini production inspection.

Fig. 23. Alumina simulant pellet with Type II shield laser welded tight around it.

A supplementary inspection technique to confirm the presence of benign geometric reflectors was developed and used for Cassini production inspection. This technique is tangential radiography (RT), which was developed at WSRC. This method involves making one or more tangential x-ray exposures of the circumferential portion of a capsule that shows a rejectable UT indication. The setup for this test is shown schematically in Fig. 24. Because each type of

Fig. 24. Tangential X-ray of Cassini capsule.

geometric reflector has a unique profile, as illustrated in Fig. 6*(a)*–(*c*), they are easily identifiable with high-resolution radiography.

The initial development work was carried out using a ^{192}Ir gamma ray source. Test capsules contained depleted $^{238}UO_2$ simulant fuel pellets. The resolution achieved was able to provide definitive characterization of the reflectors that had produced the UT signals. The technique was transferred to LANL where a 24-MeV betatron was used as the x-ray source. Because of the betatron's higher energy, better monochromaticity, and longer source-to-film distance, image resolution was even higher than that achieved at WSRC. This technique was implemented for all supplemental x-ray inspections during Cassini production.

Internal mismatch, shown in Fig. 6(*b*), was as prevalent as weld shield fusion. This is not surprising in view of the fact that all cladding cups had deformation texture-driven wall thickness variations. In addition, because the cup manufacturing process (vent slot placement) intentionally offset the crystallographic texture of the vent cup 90° from that of the shield cup, 100% of the capsules had some degree of internal mismatch prior to welding. This is borne out by the fact that it has been reported[10] that the attribute with the greatest variation throughout cup production was the wall thickness in the closure weld zone. Because, as discussed above, the degree of overpenetration was necessarily limited, the configurations of the quasi-corners produced by the mismatch varied in a complex and unpredictable way. Thus, the strength of the reflected UT signal also varied. RT proved to be highly effective in identifying internal mismatch, which produced reject-level signals in standard UT scans.

The final benign geometric reflector, internal concavity/external bulge, shown in Fig. 6(*c*), existed to some extent on all the Cassini capsules. The location was usually in the 0°–90° quadrant, and the presence of the external bulge was detectable by visual inspection. If the corners along the edges of the internal concavities that accompany the bulges are sharp enough, they can be strong geometric reflectors. Generally, however, bulges that pass the ring gage do not have concavities that produce reject-level UT signals. In any case, RT can easily identify the severity of the concavity corners and even measure the wall thickness in the bulged area.

An example of some of the geometric reflectors that must be dealt with is shown in Fig. 25. This is a replication of the inner surface of an early weld development capsule (WT-9). It shows

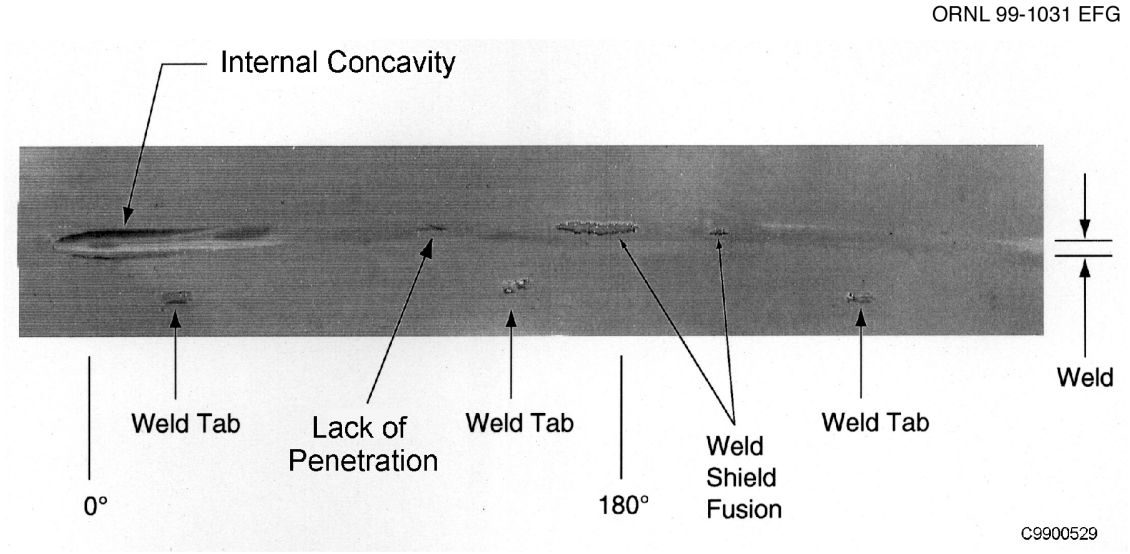

Fig. 25. Replica of the inside surface of the girth weld in capsule WT-9.

a deep internal concavity associated with a large external bulge, a short area of lack of penetration, and two areas of weld shield fusion. Each of the weld shield fusions shows a "nugget" that tore out of the weld shield when it was removed from the capsule. The three locations marked "weld tab" are remnants of the weld shield removal and do not figure in the girth weld NDE. The UT inspection results for this capsule are given in Table 4.

Note that the only reject-level (greater than 0.00512 equivalent in.) signal was produced by the tie-in concavity. The OD bulge associated with the concavity resulted in an OD of 30.36 mm, too large to pass the 30.226-mm ring gauge, and the weld thickness in the bulge was a rejectable 0.318 mm.

Table 4. UT inspection results for capsule WT-9

Vent cup position	Peak signal (equiv. mm)	Location (deg.)	Flaw type[a]
Down	0.241	6	Tie-in concavity
Down	0.117	170–185	WSF
Down	0.104	123	LOP
Down	0.066	216	WSF

[a]WSF = weld shield fusion; LOP = lack of penetration.

5. PRODUCTION INSPECTION

The NDE of the girth welds in the flight-quality GPHS capsules involved a sequence of five separate inspections. Each of these inspections is described below in its order of application.

1. Visual inspection in the welding fixture—Immediately after welding, the girth weld was visually examined for defects as the capsule was rotated in the welding fixture. The primary cause of rejection at this stage was weld blowout. Other characteristics, such as surface undercut and excessive variation in weld width, were noted.

2. Ring gauge go/no-go inspection—After it was unloaded from the welding fixture, but while still in the glove box, each capsule was passed through a ring gauge. The weld OD must be less than 30.226 mm for the capsule to pass the gauge successfully.

3. Helium leak testing—After the capsule was removed from the glove box and decontaminated, it was subjected to a helium leak test. The leak rate must be less than 1.0×10^{-6} cc-atm/s.

4. Ultrasonic testing—Automated UT, using the top-scan method, followed leak testing. Test data were presented in C-scan format with signal amplitude converted by system software to equivalent mil crack depth. The rejection level was 0.13 equivalent millimeter (5.12 equivalent mils). Two ultrasonic scans were made on each capsule, one from each end.

5. Tangential radiography—Any capsule that was rejected by UT was subjected to RT in the location(s) of the rejectable UT signal(s). The radiography results were evaluated to determine whether the UT signals were reflected from benign geometric anomalies.

6. B-Scan analysis—For capsules that were rejected by standard UT, B-scan data files were generated. These files were forwarded to the Y-12 Plant for interpretation regarding the distance of the reflector(s) from the weld centerline.

6. PRODUCTION INSPECTION RESULTS

6.1 VISUAL INSPECTION

The rejectable defects encountered during visual inspection of the capsules in the welding fixture were 1 unacceptably narrow weld and 11 weld blowouts. The blowouts were caused by a buildup of gas pressure inside the capsule because of the heat generated during welding. Normally, this pressure is released through the vent slot adjacent to the weld starting position. It appears that the drawing dimensional tolerances permitted vent slots that were marginal in area for the stated purpose, thereby resulting in weld blowouts.

During the latter stages of production, 64 capsules (FC0205–FC0214 and FC0262–FC0316), which had enlarged notches in the shield cups, were welded. The notches were widened from the original nominal 0.25/0.35-mm to a nominal 0.45/0.60-mm width. Only one of these capsules, FC0262, suffered a blowout. Subsequent to the end of production, a study[11] was performed with the objective of optimizing the vent slot areas for future heat source capsules.

The capsules that failed visual inspection are listed in Table 5. It was possible to reuse 10 of the 12 fuel pellets loaded into these failed capsules. The scrapped pellets were too extensively fractured to be reused.

Table 5. Visual inspection rejections[a]

Capsule No.	Cause of rejection	Disposition
FC0011	Very narrow weld	PNR
FC0015	WB	PNR
FC0066	WB	PR/FC0070
FC0099	WB	PR/FC0102
FC0130	WB	PR/FC0136
FC0159	WB	PR/FC0168
FC0184	WB	PR/FC0183
FC0185	WB	PR/FC0187
FC0193	WB	PR/FC0197
FC0204	WB	PR/FC0218
FC0262	WB	PR/FC0264
FC0308	WB	PR/FC0316

[a]PR/FCxxxx—Pellet reused in FCxxxx; PNR—Pellet not reusable; WB-Weld blowout.

6.2 RING GAUGE INSPECTION

The capsules that failed the ring gauge inspection did so because of unacceptable weld bulges. These bulges were usually in the weld tie-in area, that is, the 0°–90° quadrant. However, no available data detail the exact location and circumferential extent of each bulge. Because of

the vent slot area problem discussed above, it is conceivable that some of the bulging could have been caused by pressure build-up prior to weld tie-in (when the vent slot is closed). If such were the case, bulging would also be seen in the 270°–0° quadrant. The capsules which failed the ring gauge inspection are itemized in Table 6. Once again, all but 3 of the 20 pellets were extracted from the failed capsules in a reusable condition.

Table 6. Ring gauge rejections[a]

Capsule No.	Disposition
FC0055	PR/FC0068
FC0057	PR/FC0075
FC0059	PR/FC0076
FC0067	PNR
FC0069	PR/FC0072
FC0085	PR/FC0087
FC0090	PR/FC0101
FC0116	PR/FC0122
FC0131	PR/FC0143
FC0136	PR/FC0144
FC0142	PR/FC0082
FC0147	PR/FC0148
FC0161	PR/FC0167
FC0168	PR/FC0169
FC0175	PR/FC0177
FC0180	PR/FC0182
FC0227	PNR
FC0230	PR/FC0226
FC0236	PNR
FC0254	PR/FC0255

[a]PR/FCxxxx—Pellet reused in FCxxxx; PNR—Pellet not reusable.

6.3 HELIUM LEAK TESTING

Only one capsule, FC0166, failed the leak test. This failure resulted from a decontamination cover that leaked rather than a defect in the girth weld. Because of a concern that the pellet might have been affected during the preleak test decontamination, the pellet was scrapped per a Department of Energy (DOE) directive.

6.4 ULTRASONIC TESTING

Of the 317 capsules that were fabricated, 284 were subjected to UT. The testing was performed from both ends of each capsule using the top-scan technique described previously. As detailed in Table 7, 44 capsules were rejected by UT for having reflector sizes in excess of

Table 7. Ultrasonic test rejections

Capsule No.	UT reflector details[a]
FC0005	0.145 @ 230°
FC0008	0.140 @ 180°
FC0024	0.208 @ 16°
FC0025	0.221 @ 134°; 0.157 @ 165°
FC0026	0.203 @ 130°; 0.137 @ 200°
FC0030	0.231 @ 131°; 0.160 @ 186; 0.140 @ 234°
FC0034	0.178 @ 276°
FC0036	0.152 @ 224°; 0.163 @ 265°; 0.191 @303°; 0.150 @ 315°
FC0037	0.155 @ 174°; 0.180 @ 201°
FC0040	0.216 @ 126°; 0.152 @ 220°, 0.163 @ 290°
FC0041	0.203 @ 108°; 0.168 @ 270°
FC0045	0.137 @ 162°; 0.155 @ 220°
FC0048	0.152 @ 270°
FC0049	0.140 @ 205°
FC0050	0.173 @ 107°; 0.142 @ 124°
FC0053	0.193 @ 31°
FC0056	0.137 @ 195°
FC0062	0.135 @ 112°
FC0065	0.150 @ 240°
FC0071	0.173 @ 210°; 0.165 @ 240°
FC0076	0.160 @ 280°; 0.137 @ 320°
FC0080	0.206 @ 243°; 0.198 @ 293°
FC0081	0.135 @ 260°; 0.157 @ 285°; 0.150 @ 350°; 0.150 @ 352.5°
FC0089	0.140 @ 82°
FC0120	0.135 @ 88°; 0.135 @ 100°
FC0134	0.157 @ 115.5°; 0.234 @ 140°
FC0149	0.234 @ 85°; 0.183 @ 159.5°
FC0182	0.173 @ 135°
FC0188	0.226 @ 271.5°; 0.231 @ 287°
FC0190	0.150 @ 213°
FC0197	0.196 @ 295.5°; 0.163 @ 320.5°
FC0208	0.236 @ 70.5°; 0.152 @ 93°; 0.229 @ 135°
FC0212	0.155 @ 18°
FC0234	0.137 @ 44.5°
FC0273	0.236 @ 130°

Table 7. (continued)

Capsule No.	UT reflector details[a]
FC0282	0.142 @ 64°
FC0286	0.147 @ 18°
FC0289	0.140 @ 262°
FC0296	0.140 @ 289°
FC0301	0.203 @ 67°
FC0307	0.150 @ 182°
FC0328	0.236 @ 40°; 0.135 @ 56°; 0.236 @ 68°; 0.147 @ 98°
FC0334	0.157 @ 250°
FC0338	0.168 @ 73°

[a]Reflector size in equivalent millimeters; angular location in degrees from weld start.

0.13 equivalent mm (5.12 equivalent mils). These results represent a 15.5% rejection rate, obviously not a situation to be desired.

Because, as discussed above, the production UT technique was unable to discriminate between harmful discontinuities and benign anomalies, supplementary testing was performed on the rejected capsules.

6.5 B-SCAN ANALYSIS

The UT data from 21 rejected capsules were submitted to the Y-12 Plant personnel for B-scan analysis. Of these 21 capsules, 13 capsules (61.9%) were deemed to be acceptable with their reflectors identified as either weld shield fusion or internal mismatch. Two capsules (9.5%) were interpreted to have possible cracks. However, metallographic confirmation of this judgment was never made. The remaining six (28.6%) capsules were tentatively interpreted to have internal mismatch. This judgment was later confirmed by RT in five cases, and in the sixth case the call was changed to weld shield fusion. The B-scan analysis results are presented in Table 8.

Table 8. Supplementary test results[a]

Capsule No.	Y-12 B-scan analysis	Tangential radiography	Disposition
FC0005	A-WSF	A-WSF	S/DOE
FC0008	NP	NP	LS
FC0024	PC	A-WSF	PR/FC0063
FC0025	IM	A-WSF	FQ
FC0026	NP	A-IM	LS
FC0030	IM	A-IM	FQ
FC0034	A-IM	A-WSF	FQ

Table 8. (continued)

Capsule number	Y-12 B-scan analysis	Tangential radiography	Disposition
FC0036	NP	A-WSF/IM	FQ
FC0037	IM	A-IM	FQ
FC0040	IM	A-IM	FQ
FC0041	IM	A-IM	FQ
FC0045	A-IM	A-WSF	FQ
FC0048	A-IM	A-WSF	FQ
FC0049	A-IM	A-IM	FQ
FC0050	A-IM	A-WSF	PR/FC0101
FC0053	PC	I-WSF	Rejected by Mound MRB—LS
FC0056	A-IM	A-IM	FQ
FC0062	A-IM	A-WSF	FQ
FC0065	A-IM	A-WSF	LS
FC0071	A-IM	A-WSF/IM	S/DOE
FC0076	A-IM	A-WSF/IM	FQ
FC0080	IM	A-IM	S/DOE
FC0081	A-IM	A-WSF	FQ
FC0089	A-WSF	A-WSF/IM	FQ
FC0120	NP	A-WSF	FQ
FC0134	NP	A-WSF/IM	FQ
FC0149	NP	A-WSF/IM	S/DOE
FC0182	NP	A-WSF	FQ
FC0188	NP	A-WSF	FQ
FC0190	NP	A-WSF	FQ
FC0197	NP	A-WSF	FQ
FC0208	NP	R-P	S/PNR
FC0212	NP	A-WSF	FQ
FC0234	NP	R-P	S/PNR
FC0334	NP	A-WSF	IT
FC0338	NP	A-WSF	LS

[a]A—Acceptable; LS—LANL storage; P—Porosity; R—Rejectable; NP—Not performed; WSF—Weld shield fusion; IM—Internal mismatch; PC—Possible crack; S/DOE—Scrapped per DOE directive; FQ—Shipped as flight quality; S/PNR—Scrapped, pellet not reusable; IT—Impact test.

6.6 TANGENTIAL RADIOGRAPHY

Using the technique described earlier, RT was performed on 35 of the 44 capsules rejected by the standard UT inspection. In the case of all but one (FC0008) of the nine capsules that were not radiographed, schedule constraint was the limiting factor. Of the radiographed capsules, 32

(91.4%) were deemed acceptable with reflectors being characterized as weld shield fusion and/or internal mismatch. Two (5.7%) capsules were rejected and scrapped because of porosity, and one (2.9%) capsule (FC0053) had an inconclusive interpretation of weld shield fusion. The complete RT results are also presented in Table 8.

7. PRODUCTION YIELD AND PRODUCT DISPOSITION

A summary of the production yield and the disposition of the various categories of heat source capsules is presented in Table 9. It can be seen that the overall acceptance rate for flight-quality (and upgraded) capsules was 80.4%. This represents an improvement of 7.7 percentage points over the Galileo/Ulysses performance.

Table 9. Summary of capsule production yields

Capsules welded and inspected	317	
Capsules with no discrepancies shipped as flight quality	203	64%
Capsules with initial UT rejection upgraded to flight quality	22	6.9%
Capsules with no discrepancies diverted to nonmission use	26	8.2%
Capsules with initial UT rejection and subsequent upgrade diverted to nonmission use	4	1.3%
Nonupgraded capsules diverted to nonmission use	3	0.9%
Capsules scrapped with reusable fuel pellets	38	11.9%
Capsules and pellets scrapped	21	6.6%
Clads scrapped as total loss	59	18.6%
Pellets scrapped as total loss	21	6.6%

Table 10 shows details of the test results and fuel pellet dispositions of all the capsules that were rejected and lost to the program. Note that 17 capsules are listed in Table 10 which had acceptable girth welds and were later rejected by Program Management or, in one case, failed by mishap. This represents an additional 5.4% of yield that was lost for reasons unrelated to girth weld integrity.

Table 10. Capsule rejections and fuel pellet disposition[a]

Capsule No.	Visual	Ring gauge	Leak test	UT	B-Scan	RT	Fuel pellet disposition
FC0003	A	A	A	A	-	-	S/DOE
FC0004	A	A	A	A	-	-	S/DOE
FC0005	A	A	A	R	A	A	S/DOE
FC0015	R	-	-	-	-	-	S/PNR
FC0024	A	A	A	R	PC	A	PR/FC0063
FC0050	A	A	A	R	A	A	PR/FC0090
FC0055	A	R	-	-	-	-	PR/FC0068
FC0057	A	R	-	-	-	-	PR/FC0075
FC0059	A	R	-	-	-	-	PR/FC0076

Table 10. (continued)

Capsule No.	Visual	Ring gauge	Leak test	UT	B-Scan	RT	Fuel pellet disposition
FC0066	R	-	-	-	-	-	PR/FC0070
FC0067	A	R	-	-	-	-	S/PNR
FC0069	A	R	-	-	-	-	PR/FC0072
FC0070	A	A	A	A	-	-	Discolored clad PR/FC0232
FC0071	A	A	A	R	A	A	S/DOE
FC0075	A	A	A	A	-	-	S/DOE
FC0080	A	A	A	R	I	A	PR/FC0144
FC0082	A	A	A	A	-	-	S/DOE
FC0085	A	R	-	-	-	-	PR/FC0087
FC0090	A	R	-	-	-	-	PR/FC0101
FC0099	R	-	-	-	-	-	PR/FC0102
FC0103	A	A	A	A	-	A	S/MRB
FC0116	A	R	-	-	-	-	PR/FC0122
FC0130	R	-	-	-	-	-	PR/FC0136
FC0131	A	R	-	-	-	-	PR/FC0143
FC0135	A	A	A	N/A	-	-	Decontamination cover detached S/PNR
FC0136	A	R	-	-	-	-	PR/FC0144
FC0139	A	A	A	A	-	-	S/DOE
FC0142	A	R	-	-	-	-	PR/FC0082
FC0147	A	R	-	-	-	-	PR/FC0148
FC0149	A	A	A	R	-	A	S/DOE
FC0159	R	-	-	-	-	-	PR/FC0168
FC0161	A	R	-	-	-	-	PR/FC0167
FC0165	A	A	N/A	-	-	-	Decontamination cover detached S/PNR
FC0166	A	A	R	-	-	-	S/PNR
FC0168	A	R	-	-	-	-	PR/FC0169
FC0175	A	R	-	-	-	-	PR/FC0177
FC0180	A	R	-	-	-	-	PR/FC0182
FC0184	R	-	-	-	-	-	PR/FC0183
FC0185	R	-	-	-	-	-	PR/FC0187
FC0187	A	A	A	A	-	-	S/DOE
FC0193	R	-	-	-	-	-	PR/FC0197
FC0204	R	-	-	-	-	-	PR/FC0218
FC0208	A	A	A	R	-	R	S/PNR

Table 10. (continued)

Capsule No.	Visual	Ring gauge	Leak test	UT	B-Scan	RT	Fuel pellet disposition
FC0227	A	R	-	-	-	-	S/PNR
FC0230	A	R	-	-	-	-	PR/FC0226
FC0234	A	A	A	R	-	R	S/PNR
FC0236	A	R	-	-	-	-	S/PNR
FC0254	A	R	-	-	-	-	PR/FC0255
FC0255	A	A	A	A	-	-	Capsule damaged in heat treat; pellet on hold
FC0262	R	-	-	-	-	-	PR/FC0264
FC0273	A	A	A	R	-	-	PR/FC0280
FC0282	A	A	A	R	-	-	PR/FC0287
FC0286	A	A	A	R	-	-	PR/FC0290
FC0289	A	A	A	R	-	-	PR/FC0300
FC0296	A	A	A	R	-	-	S/DOE
FC0301	A	A	A	R	-	-	PR/FC0315
FC0307	A	A	A	R	-	-	PR/FC0314
FC0308	R	-	-	-	-	-	PR/FC0316
FC0328	A	A	A	R	-	-	S/DOE

[a]A—Acceptable; R—Rejectable; I—Inconclusive; PC—Possible crack; S/DOE—Scrapped per DOE directive; S/MRB—Scrapped per MRB directive; S/PNR—Scrapped, pellet not reusable; PR/FCxxxx—Pellet reused in FCxxxx.

Of 33 capsules diverted to nonmission use, 30 were shown to be flight quality. The inspection results and the dispositions for these capsules are shown in Table 11.

Table 11. Capsules diverted to nonmission use[a]

Capsule No.	Visual	Ring gauge	Leak test	UT	B-Scan	RT	Disposition
FC0002	A	A	A	A	-	-	NER standard
FC0006	A	A	A	A	-	-	MPMF aging study
FC0007	A	A	A	A	-	-	IT
FC0008	A	A	A	R	-	-	LS
FC0009	A	A	A	A	-	-	LS
FC0010	A	A	A	A	-	-	IT
FC0011	R	-	-	-	-	-	LS
FC0018	A	A	A	A	-	-	IT
FC0019	A	A	A	A	-	-	LS

Table 11. (continued)

Capsule No.	Visual	Ring gauge	Leak test	UT	B-Scan	RT	Disposition
FC0022	A	A	A	A	-	-	IT
FC0026	A	A	A	R	-	A	LS
FC0031	A	A	A	A	-	-	IT
FC0033	A	A	A	A	-	-	IT
FC0035	A	A	A	A	-	-	IT
FC0038	A	A	A	A	-	-	IT
FC0053	A	A	A	R	PC	I	LS
FC0065	A	A	A	R	A	A	LS
FC0086	A	A	A	A	-	A	LS
FC0253	A	A	A	A	-	-	LS
FC0322	A	A	A	A	-	-	IT
FC0327	A	A	A	A	-	-	IT
FC0329	A	A	A	A	-	-	IT
FC0330	A	A	A	A	-	-	IT
FC0331	A	A	A	A	-	-	IT
FC0332	A	A	A	A	-	-	LS
FC0333	A	A	A	A	-	-	IT
FC0334	A	A	A	R	-	A	IT
FC0335	A	A	A	A	-	-	LS
FC0336	A	A	A	A	-	-	IT
FC0337	A	A	A	A	-	-	LS
FC0338	A	A	A	R	-	A	LS
FC0339	A	A	A	A	-	-	IT
FC0340	A	A	A	A	-	-	LS

[a]A—Acceptable; R—Rejectable; I—Inconclusive; IT—Impact test; LS—LANL storage; PC—Possible Crack.

8. SUMMARY AND CONCLUSIONS

No single test could identify all the conditions found in the capsules. The automated top-scan UT procedure described in this report proved to be a sensitive and reliable method of inspection for GPHS capsule girth welds, and it identified suspect capsules for more extensive evaluation. The test was simple to set up and perform. The data management and analysis software was reliable and provided easy-to-interpret outputs. The test by itself was unable to discriminate between unacceptable planar defects such as root cracks, lack of fusion, incomplete penetration, and benign geometric anomalies such as weld shield fusion and internal mismatch. Supplementary tests were required to differentiate between the two types of indications. It is unlikely that a reasonable amount of additional development work would be successful in improving the discrimination of the standard UT technique.

The B-scan analysis of the ultrasonic signal data proved to be able to identify benign ultrasonic reflectors. It did tend, however, to classify signals as either internal mismatch or lack of fusion. Subsequent RT failed to verify any lack of fusion. Weld shield fusion was more difficult to identify, being miscalled in 57.1% of the cases later confirmed by RT. Overall, B-scan analysis was applied to 47.7% of the UT rejects. A judgment of benign reflector was made in 90.4% of the cases. Two capsules were judged to have possible cracks. One of these capsules (FC0024) was scrapped, and the other (FC0053) is in storage. The RT did not confirm a crack in either case, and no metallographic data are available from the scrapped capsule. The B-scan analysis has shown itself to be a useful supplementary tool for identifying benign reflectors; however, additional experience and/or development are required to improve its precision.

The application of artificial intelligence pattern recognition software (such as ICEPAK) to UT data analysis is theoretically capable of determining ultrasonic reflector type. However, the successful use of this approach requires that a large body of actual data, validated by destructive tests, be available for the software's "learning" mode. Due to the expense of such an undertaking for GPHS capsules, it is unlikely that this will be a practical approach to the reflector characterization problem.

The RT was shown to be highly reliable and well able to delineate benign geometric reflectors. It was performed on 79.5% of the capsules that were rejected by UT. In only one case (2.9%) was its interpretation deemed inconclusive. Tangential radiography is simple to perform, has high resolution, and provides conclusive interpretation of the nature of the questionable reflectors. Note that RT inspects only one (or two diametrically opposed) location(s) that has been previously identified by the standard UT scan. Cracks and lack of fusion, if tightly closed, would be difficult to detect by RT.

The balance of the nondestructive tests that were performed, that is, visual examination, ring-gauging and leak testing, are simple, reliable and unequivocal.

Eleven capsules, 3.5% of production, failed due to weld blowouts. This was undoubtedly the fault of an inadequate vent notch area. A subsequent study,11 aimed at optimizing vent notch size, is expected to result in future hardware that will be resistant to weld blowout.

Twenty capsules, 6.3% of production, failed to pass the ring gauge because of excessive bulging in the weld tie-in vicinity. Every production capsule had a certain degree of post tie-in bulging because internal pressure begins to build and continues to do so during weld taper, as soon as the vent notch is welded closed. The length of the weld taper is 144° (37.4 mm) past the vent notch. Of this, the weld overlap fully penetrates the initial weld pass for 51° (12.1 mm). Thus, it is apparent that some bulging is unavoidable. A subsequent cursory test has shown that a modified weld taper schedule is capable of reducing the full-penetration portion of the weld tie-in to 15° (3.8 mm) or less. This should prove to be highly effective in minimizing, or even eliminating, weld bulging. An additional factor in exacerbating bulge size is vent notch area.

Note that none of the capsules which failed the ring gauge were in the groups that had enlarged vent notches.

There were no confirmed occurrences of weld cracking. In two cases (FC0024 and FC0053), the B-scan analysis reported possible cracks. However, in both cases RT showed weld shield fusion. Improved melting practices14 for the DOP-26 material in conjunction with thorium analytical techniques with an accuracy of ±5% were successful in limiting the thorium concentration range across the program's entire DOP-26 production to 51–77 ppm (Ref. 15). Based on this experience, it may be safe to state that tie-in root cracking is a thing of the past.

RT showed that 70.6% of the capsules examined had weld shield fusions, and 41.2% had internal mismatch. It is likely that comparable proportions of the UT-acceptable capsules had the same types of reflectors. As discussed in the body of the report, the conditions leading to these two types of reflectors arise from the current manufacturing process and material of the capsules.

The processes used for Cassini production had the potential for an overall yield of 95.3% based on the following considerations:

- capsules with no discrepancies—64%
- capsules upgraded to flight quality—6.9%
- diverted capsules with no discrepancies—8.2%
- diverted upgraded capsules—1.3%
- acceptable capsules scrapped by management edict—3.8%
- capsules with avoidable weld blowout—3.5%
- capsules with avoidable bulges—6.3%
- capsules lost to avoidable mishaps—1.3%

REFERENCES

1. C. T. Liu, H. Inouye, and A. C. Schaffhauser, "Effect of Thorium Additions on Metallurgical and Mechanical Properties of Ir-0.3 Percent W Alloys," *Metallurgical Transactions*, **12**A(6), 993 (1981).

2. "Binary Alloy Phase Diagrams," Vol. 3, ed. T. B. Massalski, ASM International, 1990.

3. S. A. David and C. T. Liu, "High-Power Laser and Arc Welding of Thorium-Doped Iridium Alloys," *Welding Journal*, **61**(5), 157-s (1982).

4. W. R. Kanne, Jr., "Welding Iridium Heat Source Capsules for Space Missions," *Welding Journal*, **62**(8), 17 (1983).

5. W. R. Kanne, Jr., "Weldability of General Purpose Heat Source Iridium Capsules," p. 279 in *Proc. Fifth Symposium on Space Nuclear Power Systems*, ed. M. S. El-Genk and M. D. Hoover, American Institute of Physics, 1988.

6. D. J. McGuire, J. P. Moore, E. K. Ohriner, and G. B. Ulrich, *Production of Iridium Alloy and Carbon-Bonded Carbon Fiber Components for the Cassini Mission to Saturn*, ORNL-6933, Lockheed Martin Energy Research Corp., Oak Ridge National Laboratory, November 13, 1997.

7. J. D. Scarbrough and C. E. Burgan, "Reducing Hot-Short Cracking in Iridium GTA Welds Using Four-Pole Oscillation," *Welding Journal*, **63**(6), 54 (1984).

8. J. D. Scarbrough, "Ultrasonic Weld Examination (Single Probe)—GPHS Fueled Clad," DPSOL 235-F-PuFF-4620-A, Rev. 5, E. I. Du Pont de Nemours and Company, Savannah River Plant, November 9, 1983.

9. E. A. Franco-Ferreira and T. G. George, "Cassini Mission to Saturn Relies on Flaw-Free GTA Welds," *Welding Journal*, **75**(4), 69 (1996).

10. G. B. Ulrich and L. E. Miller, *Summary of Clad Vent Set Manufacturing Data for Cassini Mission*, Y/DV-1424, Lockheed Martin Energy Systems, Inc., Oak Ridge Y-12 Plant, June 1996.

11. G. B. Ulrich, *The Effects of Vent-Notch Area on Bulging and Thinning During the Clad Vent Set Closure-Weld Operation*, Y/DV-1425, Lockheed Martin Energy Systems, Inc., Oak Ridge Y-12 Plant, September 1996.

12. M. W. Moyer, *Ultrasonic Inspection of General Purpose Heat Source Clad Vent Set Closure Welds*, Y/DW-1310, Lockheed Martin Energy Systems, Inc., Oak Ridge Y-12 Plant, May 17, 1994.

13. A. Placr, *Ultrasonic Technique for Inspection of GPHS Capsule Girth Weld Integrity*, WSRC-TR-93-299, Westinghouse Savannah River Company, May 1993.

14. E. K. Ohriner, "Improvements in Manufacture of Iridium-Alloy Materials," p. 1093 in *Proc. Tenth Symposium on Space Nuclear Power Systems*, ed., M. S. El-Genk and M. D. Hoover, American Institute of Physics, 1993.

15. E. K. Ohriner, Private communication to E. A. Franco-Ferreira, Lockheed Martin Energy Research, Inc., Oak Ridge National Laboratory, April 1999.

ACKNOWLEDGMENTS

The authors wish to thank the following personnel for their contributions to the preparation of this report: T. G. George (LANL), E. K. Ohriner (ORNL), and G. B. Ulrich (ORNL) for technical input; J. C. Neeley (ORNL) for graphics; and C. S. Presley (ORNL) for typing.

The work described herein was conducted at

- Oak Ridge National Laboratory under DOE contract DE-AC05-96OR22464
- Oak Ridge Y-12 Plant under DOE contract DE-AC05-84OR21400
- Westinghouse Savannah River Company under DOE contract DE-AC09-89SR18035
- Los Alamos National Laboratory under DOE contract W-7405-ENG-36

INTERNAL DISTRIBUTION

1–2. E. A. Franco-Ferreira
3. E. P. George
4. E. C. Fox
5. J. F. King
6. M. W. Moyer
7. M. L. Santella
8–11. J. P. Moore
12. E. K. Ohriner
13. G. B. Ulrich
14. Central Research Library
15. Laboratory Records–RC
16–17. Laboratory Records (OSTI)

EXTERNAL DISTRIBUTION

18–25. U.S. Department of Energy, NE-50, Germantown Building, 11901 Germantown Road, Germantown, MD 20874-1290
W. J. Barnett A. S. Mehner
C. E. Brown W. D. Owings
L. W. Edgerly R. C. Raczynski
L. C. Herrera E. J. Wahlquist

26. U.S. Department of Energy, Oak Ridge Operations Office, Bldg. 4500N, Mail Stop 6269, Oak Ridge, TN 37831
S. R. Martin, Jr.

27. U.S. Department of Energy, Miamisburg Office, P.O. Box 66, Miamisburg, OH 45342
T. A. Frazier

28–29. Babcock and Wilcox of Ohio, Inc., 1 Mound Road, Miamisburg, OH 45343-3000
D. M. Gabriel
J. R. McDougal

30. Lamb Associates, Inc., 1017 Glen Arbor Court, Dayton, OH 45459-5421
E. W. Johnson

31. Lockheed Martin Astronautics, P.O. Box 8555, Philadelphia, PA 19101
R. M. Reinstrom

32–34. Los Alamos National Laboratory, P.O. Box 1663, NMT-9, MS E502, Los Alamos, NM 87545
T. G. George
E. M. Foltyn
M. A. H. Reimus

35. Orbital Sciences Corporation, Inc., 20301 Century Blvd., Germantown, MD 20874
E. A. Skrabek

36. Teledyne Brown Engineering–Energy Systems, 10707 Gilroy Road, Hunt Valley, MD 21031
M. F. McKittrick

37. Westinghouse Advanced Technology Business Area, P.O. Box 355, Pittsburgh, PA 15230-0355
    M. O. Smith

38–39. Westinghouse Savannah River Company, Savannah River Site, Aiken, SC 29808
    B. D. Howard
    A. Placr